EXCHANGE ENERGY AND POTENTIAL USING THE LAPLACIAN OF THE DENSITY

A THESIS

SUBMITTED TO THE GRADUATE SCHOOL

IN PARTIAL FULFILLMENT OF THE REQUIREMENTS

FOR THE DEGREE

MASTER OF SCIENCE

BY

CHRIS WAGNER

ADVISOR: ANTONIO C. CANCIO

BALL STATE UNIVERSITY

MUNCIE, INDIANA

MAY 2012

Abstract

THE EXCHANGE ENERGY AND POTENTIAL USING THE LAPLACIAN OF THE DENSITY

The challenge of density functional theory is the useful approximation of the exchange - correlation energy. This energy can be approximated with the local electron density and the gradient of the density. Many different generalized gradient approximations (GGA) have been made recently and there is controversy over the best overall functional.

Recent Monte Carlo simulations give evidence that the Laplacian of the density might be a better starting place than the gradient to correct the local density approximation. It also gives a better representation of the exchange potential at the nuclear cusp and of bonding between atoms. We have tested several Laplacian based GGA models for exchange for small atoms. We use known constraints on the exchange energy used in current GGA's. In many models unphysical oscillations occur in the potential, and understanding and eliminating them is part of the focus of this research. Our results suggest that smaller values for the short and long range constraints in the literature give more physically reasonable results in the Laplacian models. We also find that mixing s^2 and q seems to give a better result than only using one or the other.

Contents

List of Figures

List of Tables

Chapter 1

Introduction

1.1 Overview

Density functional theory (DFT) is a universal method to get the ground state energy of a many body system of particles without having to resort to using the Schrodinger equation. Since it is universal, it should work on whatever system we want to apply it to. The biggest difference is between the Schrodinger equation and DFT is that with many body Schrodinger equation we deal with a many body wave function for the system. When using DFT, we use the electron density, obtained using electron orbital wave functions. The electron density is much simpler to obtain than the many body wave function, as well as being quite simple to implement. Also the many body wave function has 3N coordinates, 3 spatial coordinates for each of the N particles, which makes it cumbersome to deal with. The electron density only has 3 spatial coordinates to deal with, since the different coordinates of the various orbital wave functions are all contained inside the density through a sum. DFT makes for much faster calculations than using the many body Schrodinger equation for these reasons.

In fact DFT has been so successful for modelling the ground state energy of a many

body system that one of its founding fathers, Walter Kohn, received the Nobel Prize in Chemistry for his work in its foundations [1]. Through the use of DFT, one could calculate things such as a phonons [2], semiconductor properties [3], magnetism [4], DNA [5] and quantum dots [6]. Since DFT is a universal theory, we can apply it to both macroscopic and microscopic systems, such as nanostructures. Because of the many options we are presented with in using DFT, it has been a very important step in the computational modelling of solids.

Unfortunately DFT doesn't come to us without flaws. Most things that are needed in DFT for the calculation of the energy are known either exactly or very well. However, there is one uknown in our problem: the exchange-correlation energy. The exchange-correlation energy is the energy that comes from electron-electron interactions that aren't dealt with in a static charge cloud approximation. Since we don't know how to get this exactly for every system, we must approximate it. This has lead to many different ideas as to how to approximate this energy. Today we still don't have the exact answer for the exchange-correlation energy and so we have many different ideas that don't work universally in this universal theory. We also have no way of intrisically knowing how well the calculation is doing for a particular system based on the specific approximation that has been made, and therefore we have no way of approximating the error in a calculation for an unknown system. This limits the reliability of DFT as a predictive theory. Another hiccup is that we are *only* able to calculate the ground state energy, which means we aren't able to get any excited states for the systems we're modelling.

One of the most popular attempts at approximating the exchange-correlation energy utilizes the gradient of the electron density [7–11]. The use of the gradient gives decent results, but recent Variational Monte Carlo data [12] suggests that using the Laplacian of the density will give better results than using the gradient. From

this, we have started the search for a Laplacian - based model that will give at least as good results as the gradient - based models, as well as fixing some of the downfalls of these models.

1.2 Summary of Thesis

The rest of this paper is presented as follows. Chapter 2 contains the background of DFT, discussing its beginning and development as well as details for why to do this research. Chapter 3 discusses the methodology of our research, including the systems and codes we used. Chapter 4 gives a layout of the results that we found from the many ideas that we tried. Chapter 5 has our final conclusions about our findings and some ideas about what can be done in the future.

Chapter 2

Background

2.1 Thomas - Fermi Theory

In 1927, Thomas and Fermi had the idea that it would be possible to approximate the energy of a system of particles using the density of electrons in a system [13]. This was a very simplistic model, completely ignoring the exchange and correlation interactions between the electrons. The Thomas-Fermi energy was given by [14]:

$$E_{TF}[n] = T_{TF}[n] + E_{ne}[n] + E_H[n] \tag{2.1}$$

where T_{TF} is the Thomas-Fermi kinetic energy created using the homogeneous electron gas (a sea of electrons that has the same density of electrons for all space), E_{ne} is the energy from electron-nucleus coulomb attractions and E_H is the Hartree energy for static electron-electron repulsions [15]. These are given by:

$$T_{TF}[n] = \frac{3(3\pi^2)^{2/3}}{10} \int n^{5/3}(\mathbf{r}) d^3r \tag{2.2}$$

$$E_{ne}[n] = \sum_a \int \frac{N_a n(\mathbf{r})}{|\mathbf{R}_a - \mathbf{r}|} d^3r \tag{2.3}$$

$$E_H[n] = \frac{1}{2} \int \int \frac{n(\mathbf{r}) n(\mathbf{r}')}{|\mathbf{r} - \mathbf{r}'|} d^3r d^3r' \tag{2.4}$$

Because of the way each of these terms is determined (Eqs. (2.2), (2.3), (2.4)), this is calculated for only a few points in space, making it quite efficient. Since no concept of dynamic interactions was included by Thomas and Fermi, Dirac added an exchange term for the homogeneous electron gas [14]:

$$K_D = \frac{3}{4} \left(\frac{3}{\pi} \right)^{1/3} \int n^{4/3}(\mathbf{r}) d^3r \tag{2.5}$$

Subtracting this from the Thomas-Fermi energy gives the Thomas-Fermi-Dirac equation. Before continuing, it is important to note that correlation is still not included in this equation and we are presented with an incomplete equation.

2.2 The Basis For Density Functional Theory

After Thomas and Fermi, not much thought was put into finding the energy by using the density of electrons until two people came and made it worthwhile. Hohenberg and Kohn published a paper in 1964 [16] which was part of what started the field of density functional theory. This paper has thousands of citations. The most important ideas in this paper are the two theorems which they stated.

The first theorem simply states that there is a one to one mapping between the ground state electron density $n_0(\mathbf{r})$ and an external potential $V_{ext}(\mathbf{r})$. If we have $n_0(\mathbf{r})$, then we can find the $V_{ext}(\mathbf{r})$ associated with it or vice versa. This can be easily shown using the variational theorem.

The second theorem states that if we have the total energy and minimize it with

respect to the density for a given external potential $V_{ext}(\mathbf{r})$, then that minimum energy will be the ground state energy E_0 (global minimum energy) and the density associated with that energy is the ground state density $n_0(\mathbf{r})$.

Proofs of these theorems are given by Martin [15]. To see the proofs refer to Ch. 6 of his book.

2.3 Implementation: The Kohn - Sham Equation

Kohn and Sham tried to solve an auxiliary problem to the problem suggested by Hohenberg and Kohn. The problem stated by Hohenberg and Kohn was that if we knew the external potential, then we would be able to get the ground state density through a minimization process of a many-body interacting system. Since this is very difficult to do, the auxiliary problem uses the ansatz that we can use a *non-interacting* system that produces a *non-interacting* density, which then is equal to the ground state density [17]. By creating this auxiliary problem, we can then write our Hamiltonian as such:

$$\hat{H}^{\sigma}_{aux} = -\frac{1}{2}\nabla^2 + V^{\sigma}_{eff} \tag{2.6}$$

where the first term is the kinetic energy and the second term is an effective local potential that affects an electron located at a point in space $\mathbf{r}$ and having a spin σ. Notice Eq. (2.6) is an independent particle equation.

We are able to express the electron density as a sum using the electron orbital wave functions after solving Eq. (2.6) [15]:

$$n(\mathbf{r}) = \sum_{\sigma} n(\mathbf{r}, \sigma) = \sum_{\sigma} \sum_{i=1}^{N^{\sigma}} |\psi^{\sigma}_i(\mathbf{r})|^2 \tag{2.7}$$

Kohn and Sham wrote the energy functional equation as:

$$E_{KS} = T_s[n] + \int dr V_{ext}(r)n(r) + E_H[n] + E_{II} + E_{xc}[n] \tag{2.8}$$

where T_s is the kinetic energy, V_{ext} is the potential created from nucleus-electron interactions, E_H is the Hartree energy associated with an electron's interaction with a static charge cloud, E_{II} is energy from ion-ion interactions (which by definition does not affect the electrons) and E_{xc} is the exchange-correlation energy. The exchange-correlation energy has been chosen to satisfy our independent non-interacting particle problem such that the non-interacting energy is the same as the ground state energy of the original problem. Unfortunately this means that the exchange-correlation energy is the only term not known exactly. This energy will be discussed more in Section 2.4. The kinetic energy $T_s[n]$ is directly related to the orbitals [15]:

$$T_s = -\frac{1}{2}\sum_{\sigma}\sum_{i=1}^{N^\sigma}\left\langle \psi_i^\sigma|\nabla^2|\psi_i^\sigma\right\rangle = \frac{1}{2}\sum_{\sigma}\sum_{i}^{N^\sigma}\int d^3r|\nabla\psi_i^\sigma(\mathbf{r})|^2 \tag{2.9}$$

In this auxiliary problem, we are able to go backwards to get the Hamiltonian from this energy. If we do, then we can compare our potential to V_{eff}^σ from Eq. (2.6). We can do this through a minimization of the Kohn - Sham energy [15]. Since $T_s[n]$ is explicitly dependent on the orbitals, we can get a variational derivative for the energy, with respect to orbitals:

$$\frac{\delta E_{KS}}{\delta\psi_i^{\sigma*}(\mathbf{r})} = \frac{\delta T_s}{\delta\psi_i^{\sigma*}(\mathbf{r})} + \left[\frac{\delta E_{ext}}{\delta n(\mathbf{r},\sigma)} + \frac{\delta E_H}{\delta n(\mathbf{r},\sigma)} + \frac{\delta E_{xc}}{\delta n(\mathbf{r},\sigma)}\right]\frac{\delta n(\mathbf{r},\sigma)}{\delta\psi_i^{\sigma*}(\mathbf{r})} \tag{2.10}$$

We know that the kinetic energy part and the density part are given by:

$$\frac{\delta T_s}{\delta\psi_i^{\sigma*}(\mathbf{r})} = -\frac{1}{2}\nabla^2\psi_i^\sigma(\mathbf{r}) \tag{2.11}$$

$$\frac{\delta n(\mathbf{r},\sigma)}{\delta \psi_i^{\sigma *}(\mathbf{r})} = \psi_i^{\sigma}(\mathbf{r}) \tag{2.12}$$

We also know that we have some constraints, specifically that we must have a particle (i.e. normalization of orbitals) and that these orbitals must be orthogonal:

$$\int \psi_i^{\sigma *} \psi_i^{\sigma} d^3 r = 1 \tag{2.13}$$

$$\left\langle \psi_j^{\sigma} | \psi_i^{\sigma'} \right\rangle = \delta_{ij} \delta_{\sigma\sigma'} \tag{2.14}$$

Using all of this with Lagrange multipliers, we can get the Kohn - Sham Hamiltonian type equation [14, 15]:

$$(\hat{H}_{KS}^{\sigma} - \epsilon_i^{\sigma}) \psi_i^{\sigma}(\mathbf{r}) = 0 \tag{2.15}$$

With Eq. (2.15) we know that ψ_i^{σ} cannot be zero, so that means that the parentheses with the Lagrange multipliers must be zero. We know that the Lagrange multipliers are the energies for the Hamiltonian when using various wave functions. Using Eqs. (2.6) for $\hat{H}_{KS}^{\sigma}$ and (2.10) for $\epsilon_i^{\sigma} \psi_i^{\sigma}(\mathbf{r})$ then we are able to come up with the Kohn-Sham Hamiltonian:

$$\hat{H}_{KS}^{\sigma} = -\frac{1}{2}\nabla^2 + V_{KS}^{\sigma} \tag{2.16}$$

By using the Kohn - Sham Hamiltonian with the variational Kohn - Sham energy equation (Eq. (2.10)) we can see that V_{KS}^{σ} is all the terms in the brackets. Since the only term not known exactly is the exchange-correlation term, then we have a definition for our exchange-correlation potential:

$$V_{xc}^{\sigma} = \frac{\delta E_{xc}}{\delta n(\mathbf{r},\sigma)} \tag{2.17}$$

It is important to note that when we do this calculation we start with a density

and end with a density. This means that if we want to make sure we've done the calculation correctly, we must get the same density out that we originally put in. This forces our calculations to be self-consistent.

2.4 Exchange-Correlation Energy

We noted in the last section that the exchange-correlation energy is everything else that is needed to make the non-interacting density equal the real ground state density. The big difference between the interacting many-body Hamiltonian and the Kohn - Sham Hamiltonian (not including E_{xc}) is that the interacting many-body Hamiltonian includes all of the coupling terms in it that cause the interaction between electrons. This must mean that our lumped E_{xc} can be interpreted as all the electron - electron interaction energies.

The exchange-correlation energy is actually two types of interactions combined into one: the exchange energy E_x and the correlation energy E_c.

The exchange energy comes about because of Pauli statistics. We know from quantum mechanics that when two electrons have the same spin, they are not allowed to occupy the same location in space, although this is possible for two electrons of opposite spin. This creates an effective hole around the electron, called an exchange hole. Because of this, there is some change in the electrostatic energy associated with the fact that two particles are in particular spin states and this change in energy is known as the exchange energy [18]. We observe this through the Hund rules. The Hund rules state that all the electrons filling a valence shell will want to align before they start filling with opposite spins. This must mean there is some favor in energy with aligning their spins rather than opposing spins and this favor comes in through the exchange energy.

The correlation energy deals with the screening of electrons. Electrons correlate with each other in order to reduce the interaction strength between them and, therefore, reduce the energy associated with their interaction. Electrons do this by creating a hole, called the correlation hole [15]. This correlation hole acts like a positive charge around the electron so that once a second electron moves far enough away from the original, the first electron won't feel the eletrostatic effects of the second.

2.5 The Local Density Approximation

Since there is no known way of getting the exact exchange-correlation energy, an approximation must be made. For a beginning model, something simple is good. One of the simplest systems to look at is the homogeneous electron gas (HEG). We can actually find the exchange energy exactly for this system, so starting here seems like a good idea [15]. The exchange energy per particle for the HEG is given by:

$$\epsilon_x^{LDA}(r_s) = \epsilon_x^{HEG}(r_s) = -\frac{3}{4\pi}\left(\frac{9\pi}{4}\right)^{1/3}\frac{1}{r_s} \tag{2.18}$$

where r_s is the Wigner-Seitz radius given by:

$$r_s(\mathbf{r}) = \left(\frac{3}{4\pi n(\mathbf{r})}\right)^{1/3} \tag{2.19}$$

The Wigner-Seitz radius is interpreted as the smallest average distance one can travel from an electron and not encounter another electron. Note that this is the same exchange energy as used by Dirac for exchange in Eq. (2.5), since both methods use the HEG. The correlation energy per particle for the HEG cannot be obtained analytically, although a form has been given as an infinite sum. Since the correlation energy is not a focus in this research, the forms are not listed here, but can be found

in the references [15, 19].

It would be silly to approximate an entire system as having the same density everywhere, so something more clever must be done. As we expressed in Eq. (2.18), we have the exchange energy per particle in terms of r_s, which is in turn in terms of $n(\mathbf{r})$. If we can figure out how many particles are at a location $\mathbf{r}$ (i.e. if we know $n(\mathbf{r})$) then we can figure out the total exchange energy by taking the energy per particle $\epsilon_x(r_s(\mathbf{r}))$ multiply it by the number of particles per volume $n(\mathbf{r})$ and integrate over all space:

$$E_{xc} = \int n(\mathbf{r})\epsilon_x^{LDA}(r_s(\mathbf{r}))d^3r \tag{2.20}$$

This method of approximation is known as the local density approximation (LDA).

Since we have now made an assumption about how to get E_{xc}, we can now figure out how to get V_{xc} by rewriting Eq. (2.17) to fit our needs. V_{xc} given in terms of the energy density e_{xc} can be written:

$$V_{xc} = \frac{\partial(e_{xc})}{\partial n} \tag{2.21}$$

or if we write it in terms of the energy per particle $e_{xc} = n(\mathbf{r})\epsilon_{xc}$:

$$V_{xc} = \epsilon_{xc} + n\frac{\partial(\epsilon_{xc})}{\partial n} \tag{2.22}$$

This results in the exchange potential for the LDA being:

$$V_x^{LDA} = \frac{4}{3}\epsilon_x \tag{2.23}$$

The LDA is a good approximation for certain situations, specifically for slowly varying systems. Slowly varying systems can be defined in a few ways. One way

would be to have a system where the density may change by quite a bit, but it does so over a very long time and so when looking at a local area it would seem as though there is a very small change. Another way to define it is that the system may be changing its density rapidly, but the change is very small compared to the total density. Outside of these two slowly varying definitions, the LDA does not calculate correct energies, but it continues to predict good structures. Since it falls apart for systems where the density varies quickly, the next logical step would be to add the information about when it does vary quickly.

2.6 The Generalized Gradient Approximation

We now have an idea of what is needed to make the approximation better than what we have already. The next thing to figure out is how to implement it. Of course the LDA still works for the slowly varying situations, so rather than completely tossing it out, it would be a good idea to build onto it. Building onto past approximations in this way is called the Jacob's ladder strategy [20].

One thought would be to modify it with a dimensionless correction factor. We could then express the total exchange energy per particle as [7]:

$$\epsilon_x = \epsilon_x^{LDA} F_x = \epsilon_x^{HEG} F_x \tag{2.24}$$

where F_x would be the exchange enhancement factor to the HEG. When close to homogeneous systems we could return ϵ_x^{HEG} by setting $F_x = 1$. The total correlation energy uses a similar thought, but is written differently [7]:

$$\epsilon_c = \epsilon_c^{LDA} + H_c = \epsilon_c^{HEG} + H_c \tag{2.25}$$

where H_c would be the correlation enhancement factor to the HEG. The next question is what to use for an enhancement factor to produce the correct ϵ_x and ϵ_c. Various ideas of enhancement factor forms are discussed in Subsection 2.6.1.

Since we want to figure out how to enhance our system based on the inhomogeneity of the system, then perhaps looking at the local density would help. If we know the density where we are and the density around us, then we should be able to tell how inhomogenous we are. The gradient of the density $\nabla n(\mathbf{r})$ provides us with this information, which we can then compare to the total density. We must remember that we have two conditions to satisfy for our slowly-varying regions from Section 2.5. We also want to make sure that we can have a dimensionless quantity to use to make things easier on ourselves since our enhancement factor is dimensionless. To satisfy these conditions we can create a dimensionless gradient quantity [15]:

$$\mathbf{s} = \frac{\nabla n(\mathbf{r})}{(2k_F)n(\mathbf{r})} \tag{2.26}$$

where k_F is the Fermi wave vector given by:

$$k_F(\mathbf{r}) = (3\pi^2 n(\mathbf{r}))^{1/3} \tag{2.27}$$

The Fermi wave vector is the wave vector associated with the Fermi energy of the homogeneous system. Unfortunately $\mathbf{s}$ is a vector. Since the energy isn't a vector, we must square $\mathbf{s}$ to get a usable quantity:

$$s^2 = \frac{|\nabla n|^2}{(2k_F)^2 n^2} \tag{2.28}$$

By defining how we will determine the inhomogeneity of the system, we have specified the kinds of parameters that F_x will use. We know that we want to use our

dimensionless gradient variable, so $F_x(s^2)$ must be dependent on it. Also, since s^2 is dependent on the gradient that means that our ϵ_x is also dependent on the gradient and is now a functional of both the density and the gradient, $\epsilon_x(n(\mathbf{r}), \nabla n(\mathbf{r}))$

We now have the energy dependent on both the density and the gradient of the density, so we're going to have to modify our potential from the LDA in Eq. (2.22) in order to include a term that deals with our gradient. When a derivation for this new V_{xc} is done we come up with:

$$V_{xc} = \frac{\partial(e_{xc})}{\partial n} - \nabla \cdot \left(\frac{\partial(e_{xc})}{\partial \nabla n} \right) \tag{2.29}$$

which can be written in terms of the energy per particle $e_{xc} = n(\mathbf{r})\epsilon_{xc}$:

$$V_{xc} = \epsilon_{xc} + n\frac{\partial(\epsilon_{xc})}{\partial n} - \nabla \cdot \left(n\frac{\partial(\epsilon_{xc})}{\partial \nabla n} \right) \tag{2.30}$$

2.6.1 The PBE Functional and Friends

Many different ideas for functionals have been presented in the GGA category. Different ones use different ideas for obtaining the functional. Some decide that it is best to fit a functional to empirical data for one system and hope that the functional works for other systems as well. Others try to use physical concepts for creating the functionals. On the latter side, one can use properties of well known systems. Perturbation theory has been done on the HEG, and it has been shown that, for a small enough amplitude of variation (or in turn a small enough value for s^2), the dimensionless gradient variable s^2 on the HEG does a wonderful job explaining systems. The way the functional must be defined for this type of perturbed system would be:

$$F_x = 1 + \mu s^2 \tag{2.31}$$

where the μ is a constant for the small s^2 limit. There are generally two values seen used for μ: $\mu = 10/81$ and $\mu = 0.21951$. The value of $\mu = 10/81$ comes from the gradient expansion [21] and $\mu = 0.21951$ comes from experiment [7]. Unfortunately these values are not the same and so it is unknown which one is the better choice. Because of this, different values of μ are used for different functionals. Since this limit is known to work well, then we have a reason to try to include it into the creation of a funtional.

Another useful concept used is a large s^2 limit. The Lieb-Oxford bound gives a bound on the total exchange-correlation energy. The bound is defined as [22]:

$$E_{xc}[n] \geq -C \int n^{4/3}(r) d^3r \tag{2.32}$$

where $C = 1.68$. Eq. (2.32) is the known as the total integrated Lieb-Oxford bound. There is some debate as to the best value for C to bound $E_{xc}[n]$. Perdew stated a lower bound for C [23] giving $1.43 \leq C \leq 1.68$. Chan and Handy [23] have come up with a better upper limit than this of $C \leq 1.6358$. Odashima and Capelle found that through an empirical analysis of atoms, ions, molecules, solids and some model Hamiltonians (including the electron liquid, Hooke's atom and the Hubbard model) the largest value that fit everything was $C \leq 1.444$ [22]. When they only looked at ions and molecules [24] they found that the best fit was $C \leq 1.00$. This bound can be expressed as a *local* bound as well, called the local Lieb-Oxford bound [9]:

$$\epsilon_x \geq -1.68 n^{1/3} \tag{2.33}$$

The use of the local Lieb-oxford bound gives a bound on the large s^2 limit, also known as the quickly varying limit. Since the exchange energy per particle is defined as in

Eq. (2.24) and the exchange energy per particle for the HEG is defined in Eq. (2.18), then we can put a bound on F_x:

$$F_x \leq \left(\frac{4^3\pi}{3^4}\right)^{1/3} 1.68 = 2.27 \tag{2.34}$$

Because of this a functional for the quickly varying limit can be defined as:

$$F_x = 1 + \kappa \tag{2.35}$$

where κ is the quicly varying limit of the functional. The value of κ is not known specifically, but generally is chosen to satisfy the local Lieb-Oxford bound Eq. (2.33). This means that there are a variety of κ values used for various functionals. Unfortunately this can be an issue since DFT is supposed to be a *universal* theory and should use one functional to satisfy every system.

One of the GGA's used by many DFT users is the Perdew-Burke-Ernzerhof functional, abbreviated as the PBE functional. Perdew, Burke and Ernzerhof came up with enhancement factors for both the exchange energy and the correlation energy [7]. The correlation term for PBE is given by:

$$H_c^{PBE} = \left(\frac{e^2}{a_B}\right)\gamma\phi^3 \log\left(1 + \frac{\beta}{\gamma}t^2\left[\frac{1+At^2}{1+At^2+A^2t^4}\right]\right) \tag{2.36}$$

$$A = \frac{\beta}{\gamma}\left[e^{-\epsilon_c^{HEG}/(\gamma\phi^3 e^2/a_B)} - 1\right]^{-1} \tag{2.37}$$

where e is the charge of the electron, $a_B = \frac{\hbar^2}{me^2}$ is the Bohr radius, $\gamma = (1 - \log 2)/\pi^2$ is a constant, $\phi(\zeta) = [(1+\zeta)^{2/3} + (1-\zeta)^{2/3}]/2$ is a spin scaling factor, $\zeta = (n_\uparrow - n_\downarrow)/n$ is the relative spin polarization, $\beta = 0.066725$ is a constant, $t = |\nabla n|/2\phi k_s n$ is a dimensionless gradient variable and $k_s = \sqrt{4k_F/\pi a_B}$ is the Thomas-Fermi screening

wave number. This was derived from three conditions that needed to be satisfied by the correlation. Perdew, Burke and Ernzerhof mentioned that the correlation hole and exchange hole are connected and so by creating a functional for the correlation energy, they had determined a functional for the exchange. From here on, the exchange functional will only be discussed. The exchange term is given by:

$$F_x^{PBE} = 1 + \kappa - \frac{\kappa}{1 + \frac{\mu}{\kappa} s^2} = 1 + \frac{\mu s^2}{1 + \frac{\mu}{\kappa} s^2} \tag{2.38}$$

where $\mu = 0.21951$ and $\kappa = 0.804$ are the slowly varying limit and the quickly varying limit respectively, as discussed above, and s^2 is the unitless gradient variable described by Eq. (2.28). This GGA uses four specific, physical conditions to derive the enhancement factor, in which all the parameters of F_x are fundamental constants. The four conditions are density scaling, spin scaling, the gradient expansion for a slowly varying system and the Lieb-Oxford bound. Through its creation, the PBE functional incorporates the most important energy features for gradient-corrected nonlocality [7], meaning that the functional uses properties that are not local to the local gradient and density. This gives the PBE functional accurate energy calculations over the LDA and makes it one of the most energy-friendly GGA functionals. One downfall of this functional is its exchange potential when it is used in atomic systems. We can see in Fig. 2.1 that in (b) the exchange potential created by the PBE functional (the blue line) goes towards negative infinity as $r \to 0$. This is caused from the divergence term in Eq. (2.46). The radial divergence term in spherical coordinates is given by:

$$\nabla \cdot \mathbf{v} = \frac{\partial v_r}{\partial r} + \frac{2}{r} v_r \tag{2.39}$$

where v_r is the $\hat{r}$ component of $\mathbf{v}$. The reason for the blow up is because as $r \to 0$,

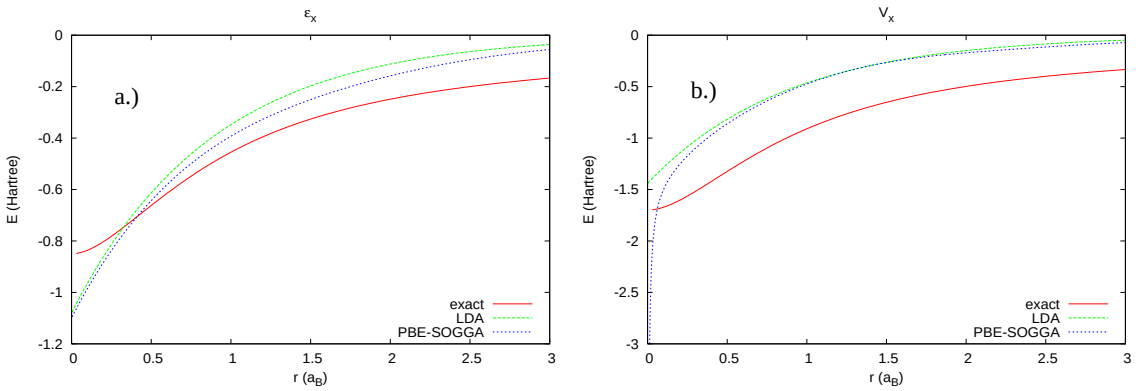

Figure 2.1: This is a graph of (a) the exchange energy per particle and (b) the exchange potential for the PBE functional. The x-axis is radial distance and the y-axis is energy, both in atomic units. The LDA and the exact curves are included for reference. The system used is the He atom. We can see that in the potential (b) for the PBE functional, there is a pole ($V_x \to -\infty$) as $r \to 0$.

$\frac{2}{r} \to \infty$.

There are many functionals that follow in the path of the PBE functional. PBEsol [8] and revPBE [9] are functionals that use the same functional form as PBE, but use different μ and κ parameters for different systems. PBEsol tries to improve the PBE functional for solids (using $\mu = 10/81$ and $\kappa = 0.804$); revPBE tries to improve the PBE functional for atomic sytems (using $\mu = 0.21951$ and $\kappa = 1.245$). The rPBE functional [10] worked with an exponential of s^2 rather than a polynomial function:

$$F_x^{rPBE} = 1 + \kappa\left(1 - e^{-\frac{\mu}{\kappa}s^2}\right) \tag{2.40}$$

This functional employs the parameters used for revPBE. The SOGGA functional [11] tries to get better results by combining the PBE functional with the rPBE functional:

$$F_x^{SOGGA} = 1 + \kappa\left(1 - \frac{1}{2}\frac{1}{1 + \frac{\mu}{\kappa}s^2} - \frac{1}{2}e^{-\frac{\mu}{\kappa}s^2}\right) \tag{2.41}$$

The parameters used for this functional are the same μ as PBEsol, but a completely

new κ value: $\kappa = 0.552$. This comes from the findings of Odashima and Capelle [24]. The many different parameters laid out here are listed in Chapter 4 in Table 4.1.

2.7 The Meta-GGA

There are ways of making approximations for the exchange-correlation energy other than just the LDA and GGA. The most recent rung of the Jacob's Ladder [20] has added a term called the kinetic energy density (KED). This kinetic energy density is defined as [25]:

$$\tau = \sum_{\sigma} \tau_{\sigma} \tag{2.42}$$

$$\tau_{\sigma} = \frac{1}{2} \sum_{i}^{occ.} |\nabla \psi_i^{\sigma}|^2 \tag{2.43}$$

where σ is the spin of an electron. Using the KED to create a meta-GGA has definitely improved on the GGA's accuracy. Unfortunately using the KED has its downfalls as well. By defining the KED as the sum in Eq. (2.43), we no longer have everything defined in terms of the density. Another issue with defining the KED this way is that it contributes to a larger calculation time (although perhaps not much larger [20]). For large systems the amount of time it takes to do a calculation is very important. Because this takes longer to calculate, sometimes people prefer to use a simple GGA over the meta-GGA.

2.8 Using The Laplacian

Similarly to the way we defined the dimensionless gradient variable s^2, we are able to define a dimensionless Laplacian variable q:

$$q = \frac{\nabla^2 n}{(2k_F)^2 n} \tag{2.44}$$

The density and Fermi wave vector (the latter defined in Eq. (2.27)) in the denominator are used to cancel out the units of the density and the Laplacian in the numerator, respectively. We know that if we end up using this Laplacian variable in a Jacob's Ladder approach, then the most complicated enhancement factor F_x that we could have would be dependent on both the gradient and Laplacian variables $F_x(s^2, q)$. Also the energy per particle could be a functional of three variables in the worst case scenario, $\epsilon_x(n(\mathbf{r}), \nabla n(\mathbf{r}), \nabla^2 n(\mathbf{r}))$. We also must take into account the fact that we have to once again modify our potential so that it can deal with a Laplacian term. When done for the energy density $e_{xc} = n(\mathbf{r})\epsilon_{xc}$:

$$V_{xc} = \frac{\partial(e_{xc})}{\partial n} - \nabla \cdot \left(\frac{\partial(e_{xc})}{\partial \nabla n} \right) + \nabla^2 \left(\frac{\partial(e_{xc})}{\partial \nabla^2 n} \right) \tag{2.45}$$

If we define it using the energy per particle:

$$V_{xc} = \epsilon_{xc} + n\frac{\partial(\epsilon_{xc})}{\partial n} - \nabla \cdot \left(n\frac{\partial(\epsilon_{xc})}{\partial \nabla n} \right) + \nabla^2 \left(n\frac{\partial(\epsilon_{xc})}{\partial \nabla^2 n} \right) \tag{2.46}$$

This has been derived from Eq. 2.17 using our definition for E_{xc} in Eq. 2.20. The extra terms were obtained using the chain rule to get derivatives with respect to the gradient and the Laplacian. Now that we have defined our dimensionless Laplacian variable and all relevant terms that go along with using it, we can see how q acts for

different systems and compare it to s^2.

2.8.1 The Gradient Expansion

One place to start thinking about the Laplacian is with a gradient expansion. When Hohenberg and Kohn did their research [16] they discussed a gradient expansion of E_{xc} and noted that in the slowly varying limit s^2 and q are equivalent up to surface terms. The equation:

$$\int n(\mathbf{r})\epsilon_x^{HEG}\left[1+\mu_s s^2\right]d^3r = \int n(\mathbf{r})\epsilon_x^{HEG}\left[1+\mu_q q\right]d^3r \tag{2.47}$$

can be shown to be true using integration by parts. Starting with the left hand of the equation, we can split up the integral:

$$\int n(\mathbf{r})\epsilon_x^{HEG}d^3r + \int n(\mathbf{r})\epsilon_x^{HEG}\mu_s s^2 d^3r \tag{2.48}$$

We can ignore the first term for now and focus on the second term. By substituting in for s^2 and ϵ_x^{HEG} using equations (2.28) and (2.18) respectively we get:

$$\int n(\mathbf{r})\left[-\frac{3}{4\pi}\left(\frac{9\pi}{4}\right)^{1/3}\left(\frac{4\pi}{3}n(\mathbf{r})\right)^{1/3}\right]\mu_s\frac{|\nabla n(\mathbf{r})|^2}{4k_F^2 n^2(\mathbf{r})}d^3r \tag{2.49}$$

Using the definition for k_F from equation (2.27) and lumping all the constants together into A we get:

$$\int A\frac{|\nabla n|^2}{n^{4/3}}d^3r \tag{2.50}$$

Integration by parts gives the integral surface and volume terms. If we make sure that we choose the correct surface, we can always make the surface terms go to zero,

so we can leave the surface terms alone and eventually get rid of them:

$$\int surface + 3A \int \left[n^{-1/3} \nabla^2 n \right] d^3r \tag{2.51}$$

If we now get rid of the surface term and focus on the volume term, we can combine things together to get $n(\mathbf{r})$ and ϵ_x^{HEG} in the numerator along with k_F^2 in the denominator. Reintroducing the integral we left out earlier we get:

$$\int n(\mathbf{r}) \epsilon_x^{HEG} \left[1 + 3\mu_s q \right] d^3r \tag{2.52}$$

We can see here that we can define a slowly varying limit for q which we shall call μ_q as to get:

$$\int n(\mathbf{r}) \epsilon_x^{HEG} [1 + \mu_q q] d^3r \tag{2.53}$$

This is quite significant. This means that for any model that utilizes a functional dependent on s^2 in the slowly varying limit, we are able to completely rewrite the functional as dependent on q using a new slowly varying constraint of $\mu_q = 3\mu_s$. This gives us a starting place to work with implementing q. We have quite a few GGA forms that use s^2 as the variable and so we could naturally switch to a form that uses q instead. At this point in time, all GGA functionals implement s^2 as the variable rather than q, so all literature values for μ are truly μ_s values and not μ_q values. This will become important in Ch 4 when we begin discussing functional forms that utilize q.

2.8.2 Prior Work with the Laplacian

Some Variational Monte Carlo (VMC) data for the Si crystal suggests that using the Laplacian might fit the total E_{xc} better than the gradient. Figure 2.2 shows (a)

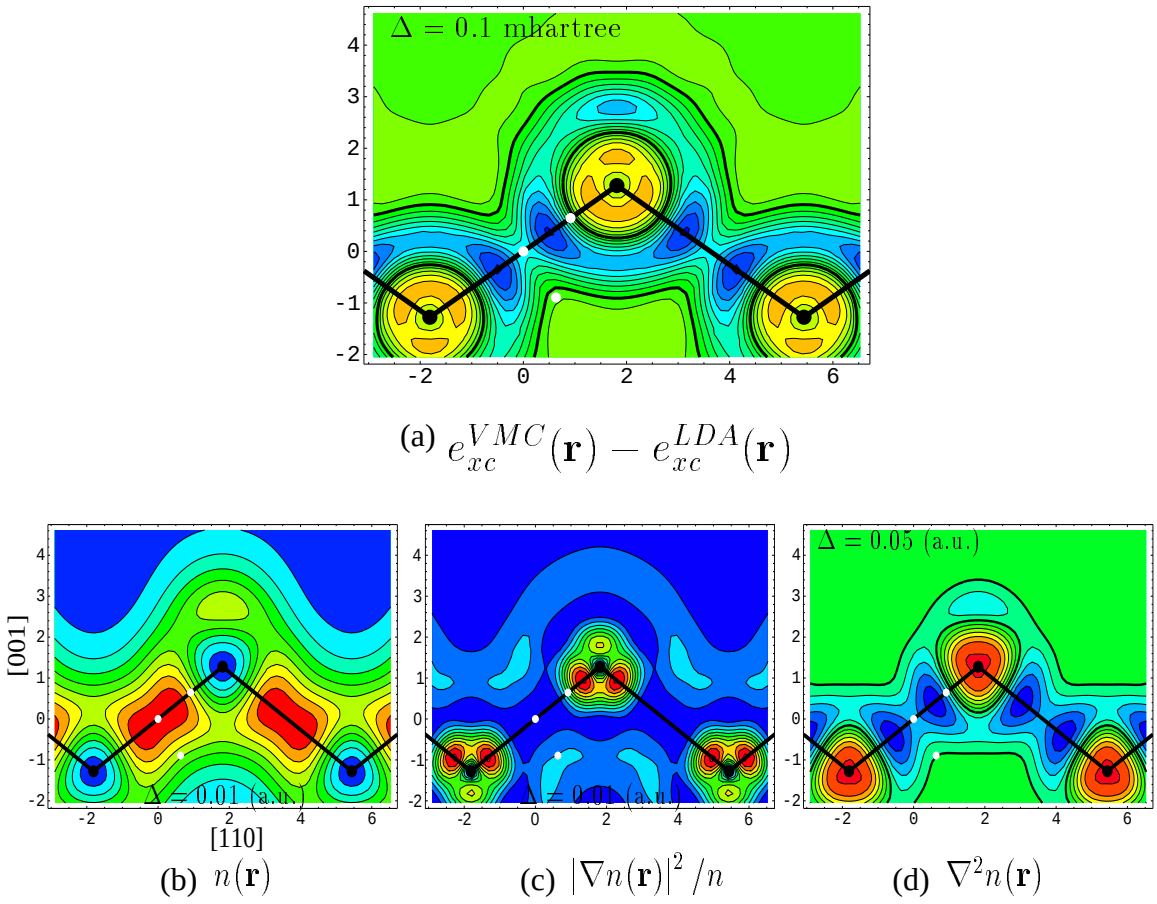

Figure 2.2: This figure shows the Variational Monte Carlo (VMC) data for Si. The plot in (a) shows the error in the LDA from the VMC data for e_{xc}. Below (a) we can see (b) the density of the Si crystal, (c) the gradient of the density squared divided by the density and (d) the Laplacian of the density. It is interesting to notice that the error in the LDA in (a) looks very similar to the plot for the Lapacian of the density in (d). This could be telling us that the Laplacian would be a good variable to use to fix the LDA model. This data set was initially found by Cancio and Chou [12]

the difference in the VMC e_{xc} and the LDA result for e_{xc}, (b) the density of the Si crystal, (c) gradient of the density squared divided by the density for the Si crystal and (d) the Laplacian of the density for the Si crystal. The work for this was done by Cancio and Chou [12]. The plot shows $\frac{|\nabla n|^2}{n}$ because it is easier to compare to $\nabla^2 n$ because of Eqs. (2.28) and (2.44). Comparing them this way they have the same units. The various colors tell us which direction (positive or negtive) the correction is being made. The thick black lines indicate a zero value, the blue regions are a positive value and the red lines are a negative value. The bluer the region is, the more positive and the redder the more negtive the error is. We note that the difference shown in (a) is error in the LDA. If we are able to add this to the LDA, then we will be able to get the correct e_{xc} for the system. Looking at the Laplacian of the data in (d) in comparison with this error in the LDA from (a), we can note that they have very similar features. The black zero lines in both aren't right on top of each other, but they are in very similar regions. The red areas near atom centers (the black dots) have very similar shapes and the blue regions along the bond (straight black line connecting the black dots) have an hourglass type of shape in both plots. It should also be noted that recent VMC calculations of e_{xc} for some small hydrocarbons also show similarities between the error in the LDA calculation and the Laplacian of the density [26–28]. The model introduced by Cancio and Chou that was tested on the Si crystal also showed promise when used on the Si atom, Mg, diamond-C and the CH_4 molecule [12]. Because of these many similarities, it would seem as though using the Laplacian of the density to fix the error in the LDA would be a good idea.

We can also compare the way the Laplacian and the gradient act in different regions of space for a specific system. The He atom is a very simple system, so we shall take a look at it. If we are to plot q and s^2 versus r, then we should be able to see the slowly varying regions for both. Figure 2.3 we are able to see $n(\mathbf{r})$, $|q|$ and

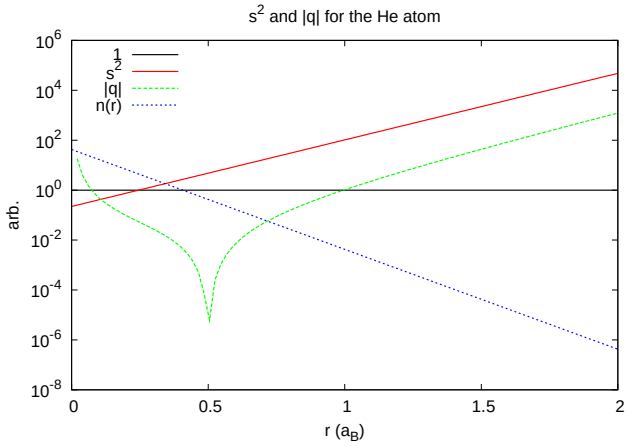

Figure 2.3: This is a figure of n, s^2, q and 1 versus radial distance for He. The x-axis is radial distance given in atomic units and the y-axis is in arbitrary units. Note that this plot is a log plot on the y-axis. The 1 that is plotted (e.g. 10^0; the black line) is to represent the place where the gradient and Laplacian variables change from slowly varying to quickly varying. We can see here that the gradient variable s^2 (the red line) recognizes the quickly-varying region as $r \to \infty$, but not as $r \to 0$. On the other hand, q (the green line) recognizes both these regions as quickly-varying.

s^2 plotted versus r. The x-axis is radial distance in atomic units and the y-axis is in unitless log values. The black line is the change from a slowly varying system to a quickly varying system, occurring at $s^2, |q| = 1$. The red line is s^2 and the green line is $|q|$. We notice that s^2 shows that the system is quickly varying outside the atom, as $r \to \infty$ and inside the atom the system is considered slowly varying. Something similar happens with $|q|$ as $r \to \infty$, although as $r \to 0$, something different happens. As $r \to 0$, $|q| \to \infty$. It is important to note that near the nuclear cusp, which is where density comes to a point at $r = 0$ and $\frac{dn}{dr}$ is discontinuous at $r = 0$, q is actually negative, which is why there is unusual behavior around $r = 0.5a_B$ (this is where $q = 0$ for the He atom). Because of the behavior near the cusp, q picks up on the fact that there is a quickly varying region right near the center of the atom. This is good, since a cusp is a quickly varying region because of the discontinuous derivative at $r = 0$. Because q picks this up and s^2 doesn't, q seems to be providing

more information about the system than s^2.

For these reasons, it seems as though using the Laplacian of the density might be a better solution than using the gradient of the density. q provides more information than s^2 and q also looks as though it is similar to the error in the LDA. We hope to be able to use q to keep the simplicity of the GGA and improve on prior GGA's accuracy without having to use the messy kinetic energy density.

Chapter 3

Methodology

3.1 Atomic Densities

As we stated in Section 3.2 the system we want to use is He. Generally in DFT the energy and density are obtained using the self-consistent method as discussed in Section 2.3. Since He is a simple system, it should be possible to get a simple, approximate model. We then don't have to go through the self-consistent method when we are prototyping our models, making the calculation simpler and faster. It's important to emphasize the fact that this model density will *only* be used for prototyping. If something looks promising, a self-consistent method will be used. Fortunately, Slater came up with simple wavefunctions and densities to use for atomic systems. The Slater model wave function [29] and density are given (respectively) by:

$$R_n(r) = r^n e^{-Z_{eff} r} \tag{3.1}$$

$$n(r) = \sum_n |R_n(r)|^2 \tag{3.2}$$

where n is the principal quantum number and Z_{eff} is a shielded nuclear charge. The shielded nuclear charge is determined by a variety of rules based on the electrons in the orbitals. The one that will concern us is the $1s$ shell for He. For the $1s$ shell, each electron shields the nuclear charge from the other with a strength of $s = 0.3$, which gives us for He:

$$Z_{eff} = Z - s = 2 - 0.3 = 1.7 \tag{3.3}$$

Since the He atom only has a $1s$ orbital this model should be very simple to implement (since we only need to incorporate $n = 1$ for He). Using the rule stated above as well as the other rules stated by Slater, Z_{eff} for Ne can also be obtained. For Ne having a nuclear charge of $Z = 10$, implementing the rules for the inner shell gives $Z_{eff} = 9.7$ and for the valence shell gives $Z_{eff} = 5.5$.

The the model density used for He are given by:

$$n(\mathbf{r}) = \frac{2}{\pi} Z_{eff}^3 e^{-2Z_{eff}r} \tag{3.4}$$

We know that the Hartree energy for this density is obtained using the pair density, as we see in Eq. 2.4. Unfortunately this contains the self-interaction of the wave functions. This self-interaxction is dealt with through the use fo the exchange energy. We can see that the self interaction term in the hartree energy (and therefore the exchange energy) is given by:

$$E_x = -\frac{1}{2} \int d^3r \int d^3r' \frac{n(\mathbf{r}) n_x(\mathbf{r}', \mathbf{r})}{|\mathbf{r} - \mathbf{r}'|} \tag{3.5}$$

where $n(\mathbf{r})n_x(\mathbf{r}', \mathbf{r})$ is the exchange pair density given by:

$$n(\mathbf{r})n_x(\mathbf{r}', \mathbf{r}) = -\sum_{\sigma} |\sum_{i}^{N_\sigma} \psi_{i,\sigma}^*(\mathbf{r}) \psi_{i,\sigma}(\mathbf{r}')|^2 \tag{3.6}$$

We can obtain ϵ_x because we have the definition of the total E_x in Eq. 2.20. By pulling out the integral over $\mathbf{r}$ and $n(\mathbf{r})$, we can produce ϵ_x. After simplification we return:

$$\epsilon_x(\mathbf{r}) = C \int d^3x' \frac{e^{-x'}}{|\mathbf{x} - \mathbf{x}'|} \tag{3.7}$$

where $\mathbf{x} = A\mathbf{r}$, $\mathbf{x}' = A\mathbf{r}'$ and $A = 2Z_{eff}$ and $C = -\frac{Z_{eff}}{8\pi}$ are constants. Through integration and reintroducing the constants it can be shown that:

$$\epsilon_x(\mathbf{r}) = -\frac{1}{2r} + \frac{1}{2}\frac{e^{-2Z_{eff}r}}{r}(1 + Z_{eff}r) \tag{3.8}$$

We were also given accurate data for V_x from Umrigar [30] for He, Be and Ne. The He data contains the radial grid r, density $n(\mathbf{r})$, exchange-correlation energy per particle ϵ_{xc} and exchange-correlation potential V_{xc} and the Be and Ne data also have the exchange potential V_x of which the most important for us is V_x. He obtained this data set through use of quantum Monte Carlo simulations. This method uses the Schrodinger equation to solve for the *exact* many particle wave function and therefore the density obtained from this wave function is exact as well. This is able to be done with quantum Monte Carlo simulations for these systems since they are simple enough to be done in a reasonable amount of time. It is then possible to do the inverse of what is normally done in DFT: take the exact density and solve for the Kohn-Sham potential such that it returns the exact density. In effect when the exact density is used, the *exact* potential is obtained. This means that by using the data we have an exact potential to compare our prototyping to. From the potential we can also obtain our exact ϵ_x. Because of this we should be able to use the data in our calculations to check our answers, or we could even include them in the code as the density for prototyping.

3.2 Noble Gases

In order to test out our thoughts on possible functionals, we must have a system to test them on. The question then becomes what system we should work with. We know that DFT is an atomistic modeling system, so it would be logical to start with an atom and work up to atomic interactions. To make sure that our thought process is correct, perhaps a simple system would be good to start with as well. In order to model either exchange or correlation energy, we must use a system that includes both of those types of energies, so that means that the H atom is out since it has only one electron. We could use the hydrogen ion H^-, but perhaps it would be best to make sure charge neutral atoms work before we get into ions.

The next thought would be He. This could be a very good system to start with. We have a model wave function for He for which the ϵ_x and V_x are able to be obtained *exactly* for a given $n(\mathbf{r})$. This is nice since it means we are able to look at how the exact answer compares to the prototypes we are testing. The model wave function is very nice to work with because it has no angular dependence. This is very helpful since it makes the gradient, divergence and Laplacian only radially dependent, getting rid of all the nasty angular terms. It is also helpful that the He atom contains regions that have q vary from negative infinity to positive infinity. The He atom also contains the nuclear cusp. Since the exchange potential gives a pole at the nuclear cusp for the PBE functional, we want to be able to fix that poor behavior. It would seem everything that has just been stated gives a good reasoning behind using the He atom to prototype various functional forms. We'll also look at Ne a bit as a check on transferability of our results.

3.3 Numerical Grid

For the calculations that we perform, everything is done on an exponential grid. The reason this kind of grid is used is because we want to get an accurate value for derivatives at different points on our grid. We know that near the nuclear cusp we want to have a fair number of points. This is because an accurate derivative of the density requires quite a few points since the gradient changes fairly rapidly right around the cusp. As we get farther and farther from the cusp, fewer points are required to get an accurate derivative, and so an exponential grid encompasses these conditions. The exponential grid that we use was implemented by Coleman and Cancio [31]. The grid is generated using the equation:

$$x_i = x_0 + dk^i \tag{3.9}$$

The grid is started at x_0 and the next point is a distance of dk away, the next point is a distance of dk^2 away, etc. The way the k value is obtained is discussed in the next paragraph. We also use numerical derivatives in the code. In order to do the numerical derivatives, a polynomial interpolator is used [32]. For N points there is one unique $(N-1)$-order polynomial that fits exactly. This means that an $(N-1)$-order polynomial is fit to a point and $\frac{N-1}{2}$ on each side of the point. Once this polynomial is fit, its derivative is calculated analytically for the center point. How we determine how many points to use is also discussed in the following paragraph.

What we want to do is choose the correct values of k and N simultaneously to minimize the error we have in our derivatives. Coleman and Cancio found what values to use for k and N by doing the error calculations for $|\nabla n|$, $r\nabla^2 n$ and $r^3\nabla^2\left(\nabla^2 n\right)$ for Xe. These were done on grids for varying values of k and a differing amount of

points for the polynomial interpolator. The smallest overall error seemed to occur for $k = 1.05$ and $N = 13$. Another common pair used is $k = 1.01$ and $N = 11$. The errors for the two are about the same, although Coleman and Cancio decided that using $k = 1.05$ fit this work best. When this was done, comparing the root mean square (RMS) error for $|\nabla n|$ from using a uniform grid with the RMS error from using an exponential grid was done. The RMS error from using the exponential grid was about 1000 times smaller than the RMS error from using a uniform grid.

3.4 Numerical Method and Code

The code *exqlapl.py* is a python code that runs prototyping simulations for exchange on atomic, radially symmetric systems. The inputs for this code are the electron density and the radial grid. The density and grid are obtained one of two ways – either the density is constructed using the Slater wave function on a grid that is created by the method described in Section 3.3, or both are input into the code using the data received from Umrigar. Once this is done, the gradient and Laplacian of the density are created. In this code, only radially symmetric cases are studied, so we only do radial parts of the gradient, divergence and Laplacian throughout the code. If the Slater wave function was used to get the density, the derivatives can be obtained analytically, and if they are data from Umrigar, they are calculated numerically using a 13 point polynomial interpolator. The routines that run these derivatives have been put into a code called *Laplacian.py*. Once we get the gradient and Laplacian of the density we are able to construct the dimensionless gradient and Laplacian terms s^2 and q.

Using s^2 and q we are able to create our enhancement factor F_x. This enhancement factor can be a function of s^2, q or both. This is performed in the code *Xqfunction-*

als.py. To do this we input whichever variable or variables are needed in the functional as well as the parameters that are used (usually μ and κ). *Xqfunctionals.py* outputs the result of F_x and also provides analytic derivatives of F_x if they were ever needed.

Now that F_x exists, we are able to create ϵ_x using Eqs. (2.18) and (2.24). At this part we are in the heart of DFT, so this part of the code is *dftheart.py*. Inside of *dftheart.py* is another code that creates ϵ_x, called *XCqnum.py*. Derivatives of ϵ_x are analytically performed here as well. These derivatives include: $\frac{\partial n\epsilon_x}{\partial n}$, $n\frac{\partial \epsilon_x}{\partial \nabla n}$ and $n\frac{\partial \epsilon_x}{\partial \nabla^2 n}$. Although each of these derivatives are used in the potential equation, part of the potential equation (2.46) is exactly the derivative with respect to the density. Because of this, the first two potential terms in Eq (2.46) are defined in *XCqnum.py* (both terms come from this derivative via the chain rule). The code *XCqnum.py* in the end outputs $n\epsilon_x = e_x$, the first two potential terms, and the other two derivatives stated above. Since this code is imbedded in *dftheart.py*, these outputs go into this code rather than the main code.

Now that we have all the derivatives needed, we can now go to *dftheart.py* to finish getting the potential. Using a 13 point interpolator, we are able to get gradients, Laplacians, gradients of the Laplacian and Laplacians of the Laplacian of the two derivative cases ($n\frac{\partial \epsilon_x}{\partial \nabla n}$ and $n\frac{\partial \epsilon_x}{\partial \nabla^2 n}$). We can see from Eq. 2.46 that for the derivative with respect to the gradient, we must do a divergence so the gradient term is necessary. Likewise we must take the Laplacian of the derivative with respect to the Laplacian for the last term in the potential equation, and so the Laplacian term is necessary. Although we have the gradient of the derivative with respect to the gradient, we still must construct the divergence. This is done simply enough:

$$\nabla \cdot \left(n\frac{\partial \epsilon_x}{\partial \nabla n} \right) = \frac{d}{dr}\hat{r} \cdot \left(n\frac{\partial \epsilon_x}{\partial \frac{dn}{dr}}\hat{r} \right) = \frac{d}{dr}\left(n\frac{\partial \epsilon_x}{\partial \frac{dn}{dr}} \right) + \frac{2}{r}\left(n\frac{\partial \epsilon_x}{\partial \frac{dn}{dr}} \right) \tag{3.10}$$

Once these terms are defined, we can define the total potential as the sum of each of the terms, where the divergence term is negative as in Eq (2.46). Since *XCqnum.py* has output e_x to *dftheart.py*, we are also able to integrate e_x over the grid to get the total integrated exchange energy E_x. This part of the code also does most of the printing. It first prints E_x once and then it prints the grid of points for r, $n(\mathbf{r})$, e_x, ϵ_x, V_x, various parts of V_x, and the gradient and Laplacian derivatives to get those parts. In the end the outputs of *dftheart.py* are e_x, V_x and E_x.

The main code also has an error analysis right at the end. The code has the ability to run completely analytic calculations for Laplacian-only enhancement factors. If this option is chosen along with the numerical calculations and the error analysis, the two methods will have an error for each point on the grid and have a mean absolute error stated at the end.

There are a few things to note about the code before moving on to discuss the results. There are quite a few things to keep track of here, so numerous flags have been applied at the beginning of the code to make checking things easy. There are many functional forms listed in the code that can be used, as well as many different parameter values. A variety of different tests have been incorporated into the code to make sure that what we think we are doing is what we are actually doing. Some of these tests do things such as check the total amount of particles and plot F_x against s^2 or q. When writing the code to perform the divergence term in the potential, an error analysis was done between the code we wrote and the result of code written by Burke for the PBE functional. When this error analysis was done, the mean absolute error was on the order of 10^{-5}. The output is very descriptive so as to make it easy to figure out to what a specific data file refers. It includes the system used (e.g. He), the nuclear charge, the occupancy of the system, what type of density is used (Slater density or Umrigar data), the name of the functional, the parameters used,

the integral of the density, a note of where the total exchange energy is listed along with the value and a list of what each column of data is for the grid before the values are listed.

Chapter 4

Results

4.1 Introduction

This chapter discusses the results we obtained from testing out various functionals using q and a combination of q and s^2. Most of the results explored used He. There were a few models that looked promising and so we tested out these functionals on Ne as well since we have the data for it. We start out with very simple models in Section 4.2 using only q. Once these were explored and failed to produce positive results, we moved on to more complex ideas incorporating both s^2 and q in Sections 4.3 and 4.4.

There are a few discussion points to make before delving into the results of this thesis work. We have many forms and parameters to discuss in this chapter. These various forms are listed in Table 5.1 along with parameters that are used in the functionals. It is worth noting that when we discuss functional forms, the exchange enhancement factor is what will be listed, although really what is being discussed and implemented is the exchange energy per particle, ϵ_x. The exchange energy per particle can be written as in Eq. (2.24), where F_x is the enhancement factor to the LDA and ϵ_x^{LDA} is given in Eq. (2.18).

Also interesting to note is that the slowly varying constraints (μ values) that we use are different than the μ values in literature. In Subsection 2.8.1 we defined a value μ_q, which is three times greater than μ_s. The μ_s was the slowly varying constraint for the functionals using s^2, which is what all the functionals in the literature use, and so the values listed in the literature are the μ_s values. Since our functionals will utilize q rather than s^2, we must use μ_q, and so we must modify the literature values to support our needs.

The final thing to discuss is figures. For each figure, the units are given in atomic units ($\hbar = m_e = e = k_e = 1$). Generally the only things that are discussed in this text are a measure of distance and a measure of energy. In atomic units the measure of distance is the Bohr radius a_B, which is the distance of a single electron in the H atom. The energy units are Hartrees, which is the same as two Rydbergs or twice the magnitude of the ground state energy of the H atom ($1Ha = 2Ry = 2|E_0^H| = 27.2eV$). Also, there are quite a few figures that use names such as PBEq-SOGGA, where two names are listed. What is meant by this name format is that the first name lists the functional used and the second name lists the parameters used. Each figure also contains the exact and LDA curves as well as what we are testing out as a comparison. The exact and LDA curves are always given by red and green lines, respectively. The reason we have an exact answer and how it is obtained is discussed in Section 3.1.

4.2 Initial Results

We started this research with two forms that we wanted to test out. The first one was the PBE functional form modified to utilize q in place of s^2. Because of the discussion we had in Subsection 2.8.1, we replaced s^2 with q as well as replacing μ (which is synonymous with μ_s since the PBE functional utilizes s^2) with μ_q. This gave us the

form:

$$F_x = 1 + \frac{\mu_q q}{1 + \frac{\mu_q}{\kappa} q} \tag{4.1}$$

Since this form has q in it in place of the s^2, we called this form the PBEq form. There are a variety of reasons for wanting to test this out. The PBE functional is utilized still today by DFT users because of its reliability with energy calculations for many systems. The PBE functional is accurate for its energy calculations, so if we want to improve the structural calculations then modifying a functional with accurate energy will hopefully produce a functional that also has accurate energy. We can see in Eq. (4.1) that at some point in space this functional will produce a pole, since q can vary from negative infinity to positive infinity, although this depends on the system for what region of space the pole is produced. This may cause problems, but it may still be informative to take a look at its results.

Another form that is of interest is similar to the PBEq form:

$$F_x = 1 + \frac{\mu_q q}{\sqrt{1 + \left(\frac{\mu_q}{\kappa}\right)^2 q^2}} \tag{4.2}$$

We call this the simple form. The real difference in this from the PBEq form is the square root in the denominator along with squaring the second term with the q. This form is interesting because including the square root along with squaring the q term in the denominator specifies the denominator to be positive for all q, completely eliminating any pole in ϵ_x. It would be reasonable to ask why the square root is in the denominator since simply squaring q makes sure the denominator is positive definite. The reason behind this is to make sure that our large q limit is still satisfied. By leaving out the square root and not squaring the $\frac{\mu_q}{\kappa}$ term, a large q limit would result in having a form that looks like:

$$F_x = 1 + \frac{\kappa}{q} \tag{4.3}$$

If this were to be the final form, we would no longer have the right large q limit as we discussed in Subsection 2.6.1 since it would be dependent on q.

4.2.1 Parameters

Before we can actually use these forms, we must determine what parameters (μ and κ values) to use inside these functionals. In the literature, there are various GGA functional forms that host a variety of μ and κ values. Table 4.1 shows different μ_s and κ values that correspond to several different GGA functionals from the literature. Since we know these parameters, we might as well use them rather than start all over finding new μ and κ values. We must first make sure to convert the μ_s values to μ_q values properly. Table 4.1 shows the conversion of μ_s from literature to the μ_q values that we need.

In GGA's, there are a variety of thoughts about what kind of parameters to use, as discussed in Subsection 2.6.1. Because of this, there are different parameter classes: hard parameters and soft parameters. The hard parameters refer to the small s^2 limit strength (i.e. μ_s) being large, and the soft parameters have a small strength small s^2 limit. Looking at Table 4.1 we can see that the hard parameters for μ_s would be from the PBE and rPBE functionals and the soft parameters would come from the PBEsol and SOGGA functionals. For us, this translates into hard and soft μ_q strengths. Of course, the κ values affect the slowly varying regions slightly, but the main contribution is from the μ_s or μ_q value.

After obtaining the μ_q and κ values, we were able to test them in the functionals mentioned in Section 4.2. When we looked at the simple functional, we produced

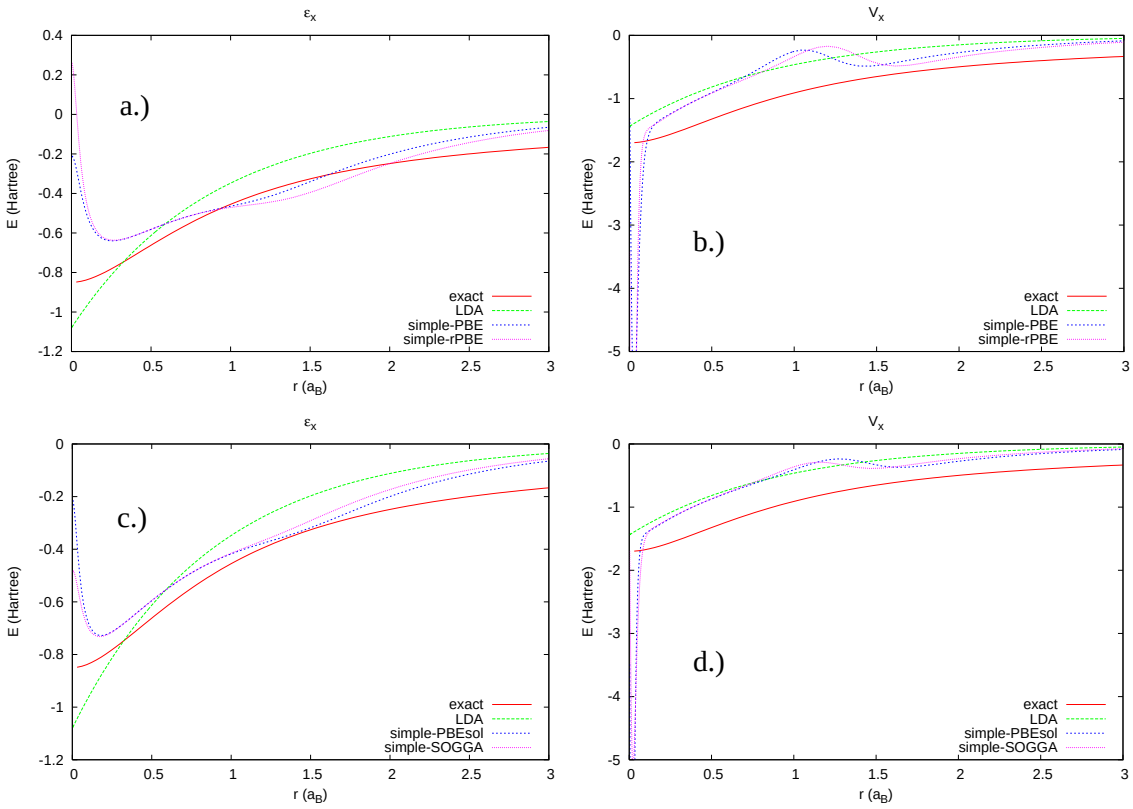

Figure 4.1: This figure shows the exchange energy per particle ϵ_x and the exchange potential V_x for the hard parameters ((a) and (b) respectively) and the soft parameters ((c) and (d) respectively) when applied to the He atom using our simple model discussed in Section 4.2.2. For each graph the x-axis is radial distance and the y-axis is energy. They are compared to the LDA curve as well as the exact curve for our Slater model density for the He atom. Note: if there are two names listed (e.g. simple-PBE) then the first name is the functional used as listed in Table 5.1 and the second is the parameters used.

Functional	μ_s	μ_q	κ
PBE	0.21951	0.64953	0.804
PBEsol	10/81	30/81	0.804
rPBE	0.21951	0.64953	1.245
SOGGA	10/81	30/81	0.552

Table 4.1: This table shows the parameters implemented by various GGA functionals. There are other functionals that also implement these combinations of μ_s and κ values, for example the revPBE functional uses the same μ_s and κ values as the rPBE funcitonal. The μ_s and κ values are found in literature and the μ_q values are simply 3 times μ_s, as discussed in Subsection 2.8.1. For more information about these functionals, refer to references [7], [8], [10], [11] respectively.

the graphs in Figure 4.1. The graphs in (a) and (c) plot ϵ_x for the hard and soft parameters, respectively, and (b) and (d) plot V_x for the hard and soft parameters, respectively. All graphs use the He atom. For every graph, the x-axis is radial distance and the y-axis is energy. In (a) we can see that as we move towards $r = 0$, the values for the simple functional go to about -0.2 and 0.2 Hartree, whereas for (c) they go to about -0.5 and -0.2 Hartree, which are much more reasonable compared to the LDA and the exact answer (discussed in Sections 2.5 and 3.1 respectively). Also, we notice that in (c) the bumps outside the nuclear cusp around $r = 1.5a_B$ are not as erratic as they are in (a), which can also be seen with the oscillation in (b) and (d). Based on what happens in (c) and (d), it would seem that the SOGGA parameters, as seen by the magenta line, produce the most desirable results for our simple functional. When working with the PBEq form, similar results were noticed, and so the SOGGA parameters were chosen for the PBEq functional as well.

4.2.2 Simple Forms

Now that we have the parameters that we want to use in Eqs. (4.1) and (4.2), we can now discuss the results of them.

Starting with the PBEq functional from Eq. (4.1) using the SOGGA parameters, we were able to produce Figure 4.2 using the He atom. Here we have plotted (a) ϵ_x and (b) V_x versus r. For both plots the x-axis is the radial distance and the y-axis is energy. As we can see from the blue line in (a), we have inserted a pole into ϵ_x that was not there before, as we discussed in Section 4.2. Unfortunately, this does not help the pole in V_x that we were originally trying to eliminate by using q in place of s^2, as the blue line in (b) shows. When we compare this to the PBE form in (b), as seen in the magenta line, the potential near the cusp seems to only have gotten

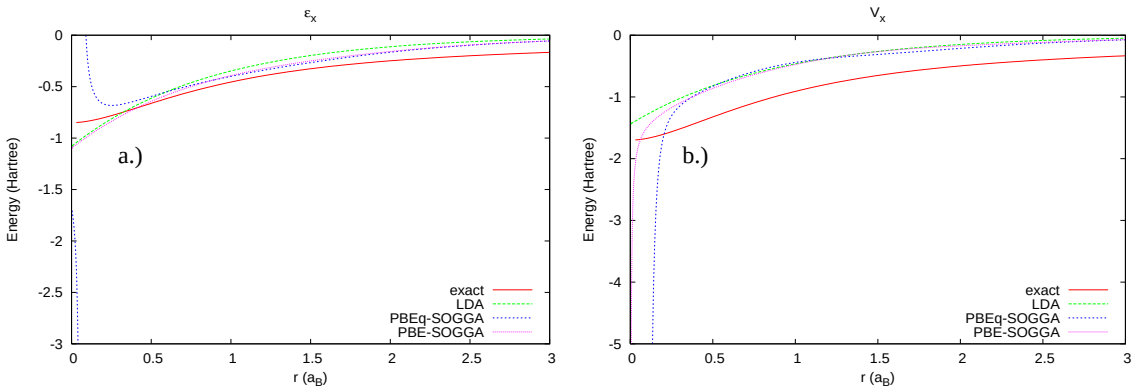

Figure 4.2: These graphs were made using the PBEq functional for the He atom. The plots show (a) ϵ_x and (b) V_x versus r. The x-axis is radial distance and the y-axis is energy. We can see in (a) that we have introduced a pole in ϵ_x. The plot of (b) shows that the pole has gotten worse (blue line) compared to the original (gradient-baased) PBE functional (magenta line).

worse.

The simple functional from Eq. (4.2) using the SOGGA parameters for the He atom gives us Figure 4.3. This has the plots of (a) ϵ_x and (b) V_x versus r. For both graphs the x-axis is radial distance and the y-axis is energy. We notice in (a) that the simple form (the blue line) takes the pole out of ϵ_x, giving us a finite value at the cusp. Unfortunately, using the square root also adds some unusual bump outside the atom around the region $r = 0.8a_B$ to $r = 2.0a_B$. This bump gets translated to V_x as an oscillation, which can be seen in plot (b) for the blue line in the same region previously stated. This can be very bad, since any further oscillations added from the density can be greatly exaggerated in V_x because of this feature, since q is very sensitive to variations in the potential.

Since these two ideas seem to have flaws in them, let's gather some ideas from everything we just observed. We know that Eq. (4.1) has a poor cusp region, even worse than the original (gradient-based) PBE form, although outside the atom everything seems to work okay. The simple form seems to have the opposite effect: outside

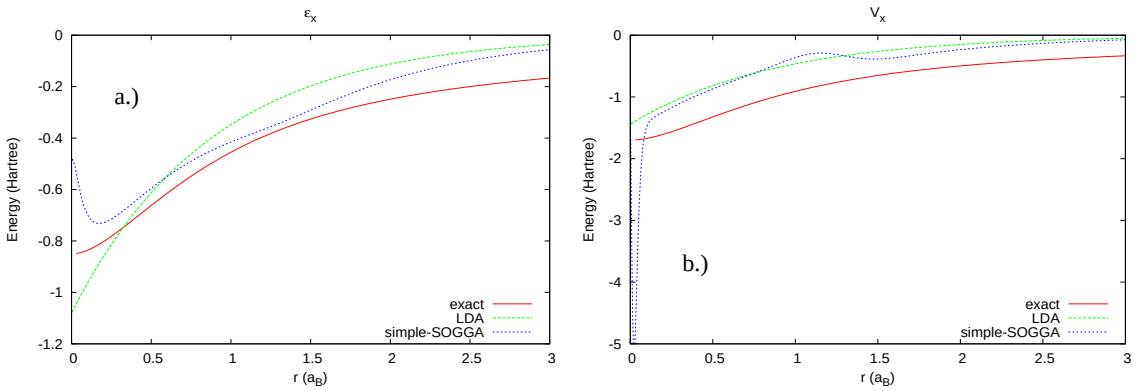

Figure 4.3: These graphs were made using the simple functional for the He atom. The plots show (a) ϵ_x and (b) V_x versus r. The x-axis is radial distance and the y-axis is energy. In (a) we see that including the square root and squaring the q term in the denominator has indeed eliminated the pole at the cusp, although it has added a bump outside the atom. Unfortunately this poor behavior outside is seen in (b) as an unphysical oscillation.

the atom has some unusual oscillations but near the cusp we have a finite value in both ϵ_x and V_x. If there is a way we can combine these two forms, then perhaps we can get the benefits of both and minimize the poor qualities of each. It would seem that we can generalize Eqs. (4.1) and (4.2) by using a form that looks like:

$$F_x = 1 + \frac{\mu_q q}{\sqrt{1 + \eta q + \left(\frac{\mu_q}{\kappa}\right)^2 q^2}} \tag{4.4}$$

where η is a switching variable. By using $\eta = 0$ we return the simple form and for $\eta = 2\frac{\mu_q}{\kappa}$ we return the PBEq form. Because this form generalizes the two forms that we currently have into one form, it was dubbed the general form.

Since we wanted to see if some kind of mix between the simple form and the PBEq form would work well, we decided that we should try to use a switching variable of $\eta = \frac{\mu_q}{\kappa}$, which would be halfway between the simple and PBEq forms. Figure 4.4 shows this switch when using the He atom. The two graphs show (a) ϵ_x and (b) V_x

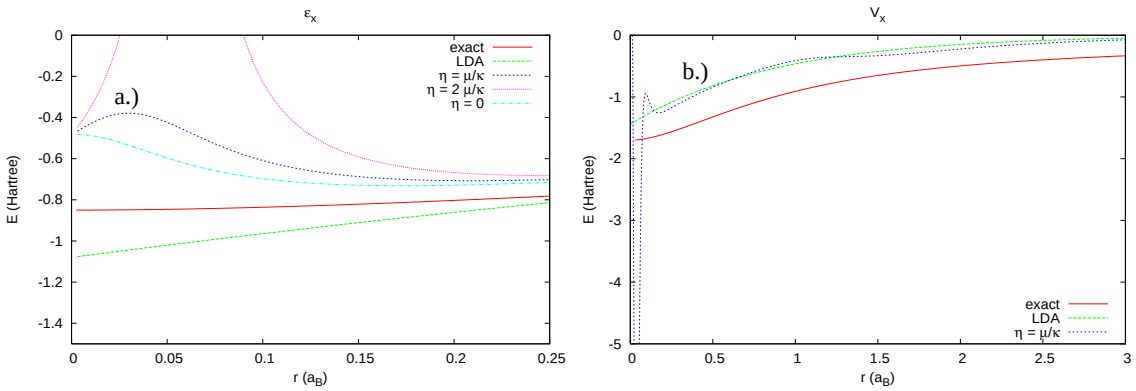

Figure 4.4: These are graphs of the switch between the PBEq and simple forms for the He atom. For both graphs the x-axis is radial distance and the y-axis is energy. We are able to see from the blue line that using $\eta = \frac{\mu_q}{\kappa}$ gets rid of the pole in ϵ_x from the PBEq form and, although not shown, it reduces the bump outside the atom. From what (b) shows us, using the η half way in between, we get a much worse cusp than we seem to get everything to be bad in V_x.

versus r for this situation. For both graphs, the x-axis is the radial distance and the y-axis is energy. In (a) we are able to see that using $\eta = \frac{\mu_q}{\kappa}$ (the blue line) gets rid of the pole near the cusp. It's not able to be seen in (a), but this value for η also reduces the bumps outside of the atom. For these reasons it looks like it would be a better form that either the PBEq or simple forms. When we look at V_x in (b) we get a whole different story. We can see that, like what happened with the simple form, the V_x contains oscillations outside the atom. Unfortunately we were not able to completely get rid of this feature, but they are better than before. The part right near the cusp is also poor. It is hard to tell, but the cusp region is finite, which is a good thing, but it isn't nearly as smooth as in the simple form. It would seem that since there is a little bump near the cusp around $r = 0.05a_B$ as the blue line in (a) shows, taking the Laplacian of it to get the potential as in Eq (2.46), it causes very large jumps in V_x. It would seem as though despite the fact that ϵ_x seems to be much better using the combination, V_x is getting all the poor qualities of each.

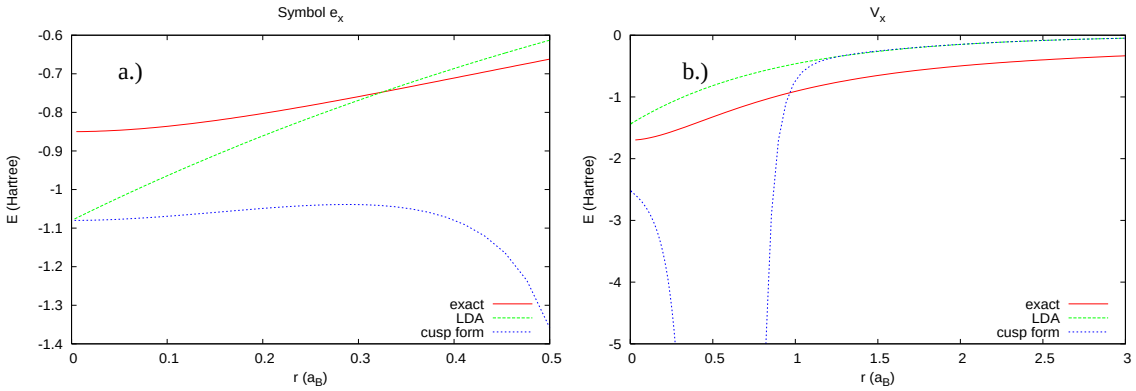

Figure 4.5: The graphs show the (a) exchange energy per particle and (b) exchange potential for the cusp form for the He atom. For both, the x-axis is radial distance and the y-axis is energy. In the exchange energy per particle (a) the features of the cusp form (blue line) match that of the exact (red line) as r goes to zero (or more specifically the derivative of ϵ_x with respect to q goes to zero as q goes to negative infinity). Unfortunately this success is overshadowed by the poor behavior of V_x as seen in (b).

One other enhancement factor that we looked at was of the form:

$$F_x = 1 + \frac{M}{q} \tag{4.5}$$

where the value used for M was $M = \frac{2}{3}s_0^2$ where s_0^2 is the value of s^2 as you approach $r = 0$. Unlike the other three forms that we have, this form looks like no other GGA or even as if it derived from other GGA's. The reason this one is interesting is because we specified the behavior at the cusp (which we will call the cusp condition): we wanted to see what would happen if we restricted the energy per particle to have the derivative with respect to r be zero as r goes to zero, or for the atomic system it would mean the derivative with respect to q would be zero as q goes to negative infinity. This would specify a nicely behaved ϵ_x at the cusp. This gave us the results for ϵ_x and V_x in Figure 4.5 for the He atom.

The graph shows (a) ϵ_x and (b) V_x for this cusp condition versus r. This means

that for both graphs the x-axis is radial distance and the y-axis is energy. We can easily see in (a) that the cusp condition is fulfilled. The blue line is the cusp form and, as always, the red and green lines are the exact and the LDA solutions respectively. We can see that the blue line follows a similar trend to the exact solution as r goes to zero. Unfortunately for this form, a pole is formed at $q = 0$, which is not easily seen in (a), although it can be seen in (b). We simply moved the pole from near the cusp to outside the atom (around $r = 0.5$ for this system). The potential is very deep, partly caused from the pole in ϵ_x.

4.3 Mixing

Unfortunately none of the forms presented in Section 4.2.2 seem to give any better results than can be obtained using a normal GGA. Since none of these seem to give any kind of desirable results, then we must move on to something else. Before we do so, it would be helpful to try to glean some information from the negative results we've gotten so far. We know that using the Laplacian gives better structural knowledge than the gradient. Based on the models that we've used so far, a lot more work will have to be done in order to simply use the Laplacian. We also know that the gradient gives desirable results, especially when trying to obtain energy information, despite the fact that it tends not to give as good structure. The next thought would be that using the two together will give a better representation of what's actually going on.

4.3.1 Motivation for Mixing

As we have shown in Section 2.8.1, s^2 and q are equivalent in the slowly varying limit. We used this equivalency to justify substituting s^2 with q inside functionals. However, this would not necessarily have to be the case. We assuumed that we could

use one or the other and get good results, although no where does it tell us that using one or the other will give the best results. Because of their equivalence it is possible that nature prefers some sort of linear combination of the two.

Because of this possibility, we proposed a mixing form that utilizes both s^2 and q. We combine them into one variable that is able to switch between the two:

$$\bar{q} = \alpha q + (1 - \alpha)\frac{s^2}{3} \tag{4.6}$$

In this case, α is the mixing variable which can vary from 0 to 1 and the 1/3 in the s^2 term comes from Eq. (2.47). When $\alpha = 0$ we return the gradient term and when $\alpha = 1$ we get back the q. Because of the way we define $\bar{q}$, whenever we discuss the slowly varying limit the μ we must use is μ_q. Of course one thing to take into account when applying this new variable to our enhancement factor is that we have multiple derivatives to deal with, some for s^2 and some for q. This was dealt with simply enough by doing the s^2 and q derivatives of $\bar{q}$ and then using the chain rule to do s^2 and q derivatives of F_x.

Before we discuss any results, it's important to note that we have many options to pick from for α values. We could pick a constant value for α or we could try to find some kind of function that varies from 0 to 1. Since picking a constant value is the simplest option, we should probably start there. Now we want to know what value to give α. Rather than floundering in the dark about this, it would probably be best to get a method to try to determine what value gives the most useful result. Perhaps we could optimize our solution somehow. We know that our very simple test case for He shows us that we don't have any unusual bumps anywhere in the exact ϵ_x. We can notice from this that there are not many features, or more specifically, there is very little curvature in ϵ_x. Because the curvature is small, perhaps we could optimize

our solutions by optimizing the curvature.

4.3.2 Optimization

In this section we discuss optimizing the curvature for various cases. Since the GGA's are based off of the LDA, a GGA curvature can be measured off of the LDA curvature. This means that a GGA curvature measure of zero would return the LDA. Since we want to try to improve on the LDA, we want to try to get some small non-zero amount of curvature. Jackson [33] tells us that if we want to get the minimum curvature of the function, then we can minimize the integral:

$$\int |\nabla\psi(\mathbf{r})|^2 d^3r \tag{4.7}$$

where $|\nabla\psi(\mathbf{r})|^2$ measures the curvature at $\mathbf{r}$. This means that we essentially have a function ψ that has minimum curvature when:

$$\nabla \cdot (\nabla\psi) = 0 \tag{4.8}$$

Since the potential has a divergence term and a Laplacian term, then we could stipulate that from the potential Eq. (2.46) we could get the curvature terms to be:

$$\nabla \cdot \mathbf{v} + \nabla^2\psi = \nabla \cdot (\mathbf{v} + \nabla\psi) = 0 \tag{4.9}$$

and we could then minimize the curvature by minimizing the integral:

$$\int |\mathbf{v} + \nabla\psi|^2 d^3r \tag{4.10}$$

if we were to square this out, three integrals would be produced:

$$\int |\mathbf{v}|^2 d^3r + \int |\nabla\psi|^2 d^3r + 2\int \mathbf{v}\cdot\nabla\psi d^3r \tag{4.11}$$

Applying this to the potential Eq. (2.46) for exchange, the $\mathbf{v}$ and $\nabla\psi$ become:

$$\mathbf{v} = -n\frac{\partial\epsilon_x}{\partial\nabla n} \tag{4.12}$$

$$\nabla\psi = \nabla\left(n\frac{\partial\epsilon_x}{\partial\nabla^2 n}\right) \tag{4.13}$$

We know that these are the terms that we want to worry about since these terms are the ones that are not included in the LDA. The integrals in Eq. (4.11) were implemented into the code using the above equations to find the minimized curvature.

Using these integrals we were able to make a choice for variables to get the best curvature. To give an idea of how this was implemented, we discuss two of the optimizations performed. This was initially implemented on the general functional to determine the best value to use for the switching variable η Eq. 4.4. Figure 4.6 (a) shows the curve to minimize the integrals. The x-axis is the η variable and the y-axis shows the value of the integral from the Laplacian part of V_x. Based on visual inspections, it seems as though $\eta = 1.6$ is the best option. In (b) we see the derivative $\nabla\frac{\partial(\epsilon_x)}{\partial\nabla^2 n}$ plotted versus r including the d^3r weighting. This means the x-axis is radial distance and the y-axis is in arbitrary units. By looking at the blue line for $\eta = 1.6$, we are able to see that this curve is quite featureless compared to the rest. Using this value seems to get rid of most of the oscillations outside of the atom.

After the optimization was done for η, we moved on to checking which α was the best choice for the general model. We just found that $\eta = 1.6$ gives the optimal result for the q only general functional. Because of this, we used this value for η

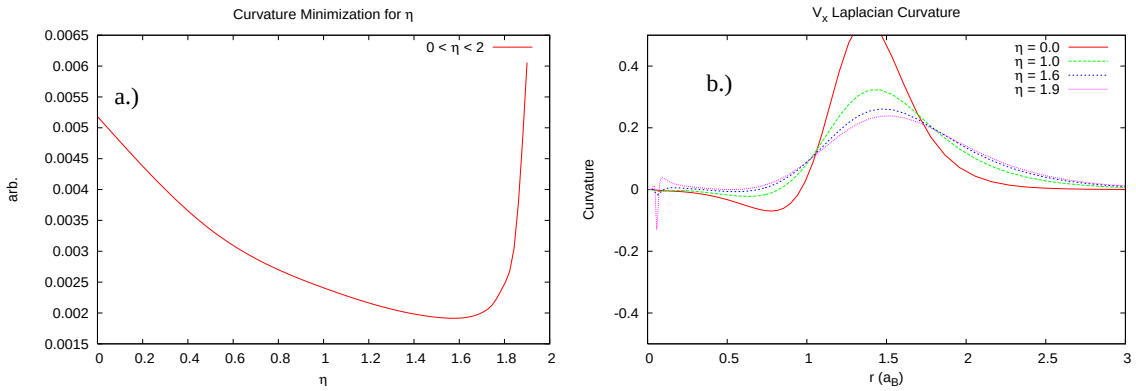

Figure 4.6: This figure shows the minimization of the curvature for η for the He atom. The plot in (a) the total integration (for this case only the Laplacian integral applies) for various values of η and for (b) there is a graph of $\nabla\frac{\partial(e_x)}{\partial\nabla^2 n}$ vs r including the d^3r weighting. For (a) the x-axis is η and the y-axis is the total integration in arbitrary units. For (b) the x-axis is radial distance and the y-axis is the curvature given by $\nabla\frac{\partial(e_x)}{\partial\nabla^2 n}$. From (a) it looks as though using $\eta = 1.6$ is the best choice for minimizing the curvature. The plot in (b) shows that $\eta = 1.6$ is rather featureless compared to the rest of the graphs. It has about the same curvature outside the atom as using $\eta = 1.9$ (close to PBEq) without nearly as extreme behavior near the cusp.

when optimizing the α value. Figure 4.7 gives the results of this optimization. As in the figure for η, Figure 4.7 (a) shows the curve of the total integration. The x-axis is the α variable and the y-axis is the integral value. The red curve is the total integration, the green curve is for the divergence, the blue curve is for the Laplacian and the magenta curve is the cross term integration in Eq. (4.11). Based on a visual inspection for the general model, the best α was right around $\alpha = 0.63$ or 0.65. In (b) we see $-n\frac{\partial(\epsilon_x)}{\partial\nabla n} + \nabla\left(n\frac{\partial(\epsilon_x)}{\partial\nabla^2 n}\right)$ versus r including the d^3r weighting for various α values. for this the x-axis is radial distance and the y-axis is given in arbitrary units. Once again, we can see the rather featureless line for the minimized $\alpha = 0.63$ value, given by the green line, compared to the other curves.

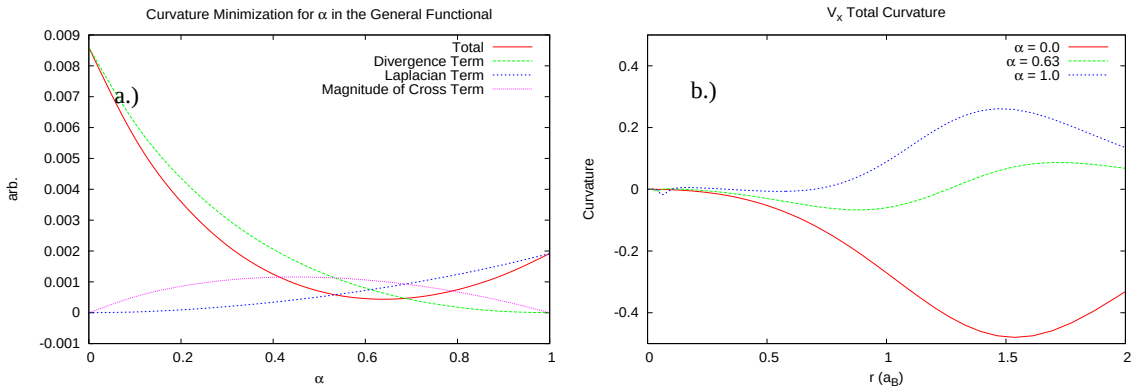

Figure 4.7: This figure shows the minimization of the curvature for α for He in the general functional after using the η found from the previous minimization. The plot in (a) the total integration along with the parts that add to the total for various values of α and for (b) there is a graph of $-\frac{\partial(e_x)}{\partial\nabla n} + \nabla\frac{\partial(e_x)}{\partial\nabla^2 n}$ vs r including the d^3r weighting. For (a) the x-axis is α and the y-axis is the total integration. For (b) the x-axis is radial distance and the y-axis is the curvature given by $-\frac{\partial(e_x)}{\partial\nabla n} + \nabla\frac{\partial(e_x)}{\partial\nabla^2 n}$. From (a) it looks as though using $\alpha = 0.63$ or so is the best choice for minimizing the curvature. The plot in (b) shows that $\alpha = 0.63$ is rather featureless (close to zero) compared to the rest of the graphs. It is important to remember that these use an r^2 weighting. Near the cusp gives some radical behavior, but outside the cusp everything is very close to zero for $\alpha = 0.63$.

4.3.3 Energy and Potential with Optimized Mixing

We tried using $\bar{q}$ in each of the enhancement factor forms mentioned in Section 4.2.2 except the cusp form. The reason the cusp form wasn't tested using the mixing factor was because of the way the cusp form was obtained as a plausible form. It was determined that to get a good form at the cusp (where the derivative with respect to r is zero as r goes to zero) we must use a form with q in the denominator and therefore using $\bar{q}$ would completely ignore that whole concept. We started by checking to make sure everything was working out by testing that $\alpha = 0$ and $\alpha = 1$ returned the proper results in each of the functionals, which came out just fine.

Starting with the PBEq functional from Equation (4.1), we varied α from 0 to 1 to try to produce the best α value. Unfortunately when doing this, the integrator gave some unusual results. Because of the pole, the value of the integration was very large, but at points the value was small. This is most likely attributed to the fact that the grid is not continuous and we may have missed the point where the pole was created. We have found smallest value for this was right around $\alpha = 0.0$ (the smallest was $\alpha = 0.05$ to be exact), essentially producing s^2 . It would seem that if there is in fact a non-zero value that best fits the PBEq functional for α, it most likely wouldn't be worth it since it will be so small the q contribution to the functional will be minimal. Also, the value that the integral produced for $\alpha = 0.05$ was only 0.002 less than the integral for $\alpha = 0$. Because of this, it would seem the best results would essentially be using the original PBE functional, more of which can be found in [7].

After figuring out that the best value for α in the simple functional is using $\alpha = 0.6$, we plugged it in and produced Figure 4.8 for the He atom. The graphs show (a) ϵ_x and (b) V_x for the simple functional with optimal mixing versus r. The x-axis is radial distance and the y-axis is energy. We see in (a) that we have reduced the bump

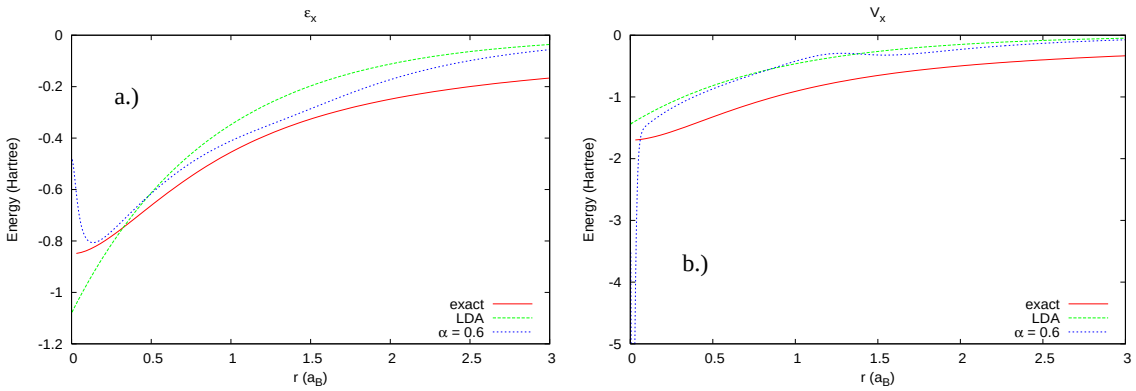

Figure 4.8: This is a graph of the simple functional for the minimized α using the He atom. In (a) we see ϵ_x and in (b) there is V_x. The x-axis is radial distance and the y-axis is energy. In (a) we are able to see that the bump outside the atom is nearly gone as well as the oscillations in (b). Also, the in (b) we can see that the bump right near the cusp is getting pushed towards $r = 0$ since the weighting of it is less there.

quite a bit, which can also be seen by the small oscillations in the potential in (b). We also notice that in (b) that the bump near the cusp is scrunched up and shoved towards $r = 0$. This helps for when it gets the r^2 weighting from the integration.

For using the general functional with $\eta = 1.6$ and $\alpha = 0.63$ as we found in Section 4.3.2 Figure 4.9 was produced for the He atom. The graphs show (a) ϵ_x and (b) V_x for the simple functional versus r. The x-axis is radial distance and the y-axis is energy. In (a) it almost looks like the bump outside the atom around $r = 1.5a_B$ isn't even there, being even smaller than the bump in Figure 4.8 (a). This can be seen in (b) as well, where the outside oscillation is nearly gone. For the cusp region, (a) has a large bump, somewhat similar to what we saw when we originally encountered this functional. This again gets translated to unusual oscillations near the cusp as seen in (b), although we keep a finite value. Similar to Figure 4.8 (b), the oscillation near the cusp gets pushed towards $r = 0$ where the weighting is less.

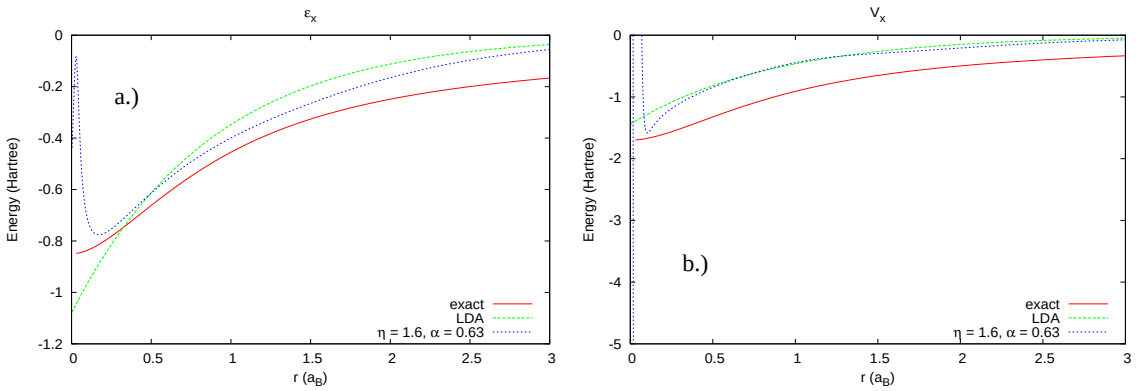

Figure 4.9: This is a graph of the general functional using the minimized η and α values. The plots contain (a) ϵ_x and (b) V_x versus r. The x-axis is radial distance and the y-axis is energy. We can see similar results with the general functional as we did with the simple functional using the minimized α. The bump outside the atom in ϵ_x in (a) is diminished, along with the oscillations in V_x in (b). The bump and oscillations near the cusp in (a) and (b) respectively are also pushed towards $r = 0$ the weighting is less.

4.4 Advanced forms

One final form that we discussed used a different coupled s^2 and q unlike what we did with $\bar{q}$. In this case we couple s^2 and q by division ($\frac{q}{s^2}$). The form was presented as:

$$F_x = 1 + \frac{As^2}{Bs^2 - q} = 1 + \frac{A}{B - \frac{q}{s^2}} \tag{4.14}$$

This functional form was discussed as a method of keeping the denominator positive definite to make sure no poles would be created when using the functional in any reasonable space. Essentially, the pole got moved to a region of the coupled s^2 and q space that isn't used. Unfortunately, this presents the issue that even though that part of space may not be used for one system, it may very well be used for another system. Thus we only redefined the problem rather than actually fixing anything in the long run. A nice side effect of this form is that it produces the cusp condition created using the cusp functional for the q goes to negative infinity limit, although

this functional was not created trying to reproduce this condition. A proper GEA is performable on this system to get the correct slowly varying limit for $s^2 \to 0$ and $q \to 0$, but has not been done as of yet. For this reason we present this form using various values for A and B.

Figure 4.10 shows the results of using this form. The plot in (a) and (b) show ϵ_x and V_x respectively for the He atom using $A = \mu_q^{SOGGA}$ and $B = 2$. Plots (c) and (d) show ϵ_x and V_x repsectively for the Ne atom using $A = \mu_q^{SOGGA}$ and $B = 2$. Plots (e) and (f) show ϵ_x and V_x respectively for the Ne atom using $A = \mu_q^{SOGGA}$ and $B = 10$. For all graphs, the x-axis is radial distance and the y-axis is energy. Both (a) and (b) produce very nice results for the He atom system that we have been using for most of this research. When we tested the functional out on Ne, the pole popped back up around the switching of $1s$ to $2s$ shell. This is able to be remedied by changing the value of B to a higher value. For example, using the value $B = 10$ we once again move the pole to a region of space that isn't being used. This originally made us suspect that making B dependent on the value of the nuclear charge Z would be able to fix the problem should it rear its head. In the end we decided that since things should be determined strictly by the density and any derivatives of the density in a universally applicable functional, the functional should not change based on the atomic system whatsoever.

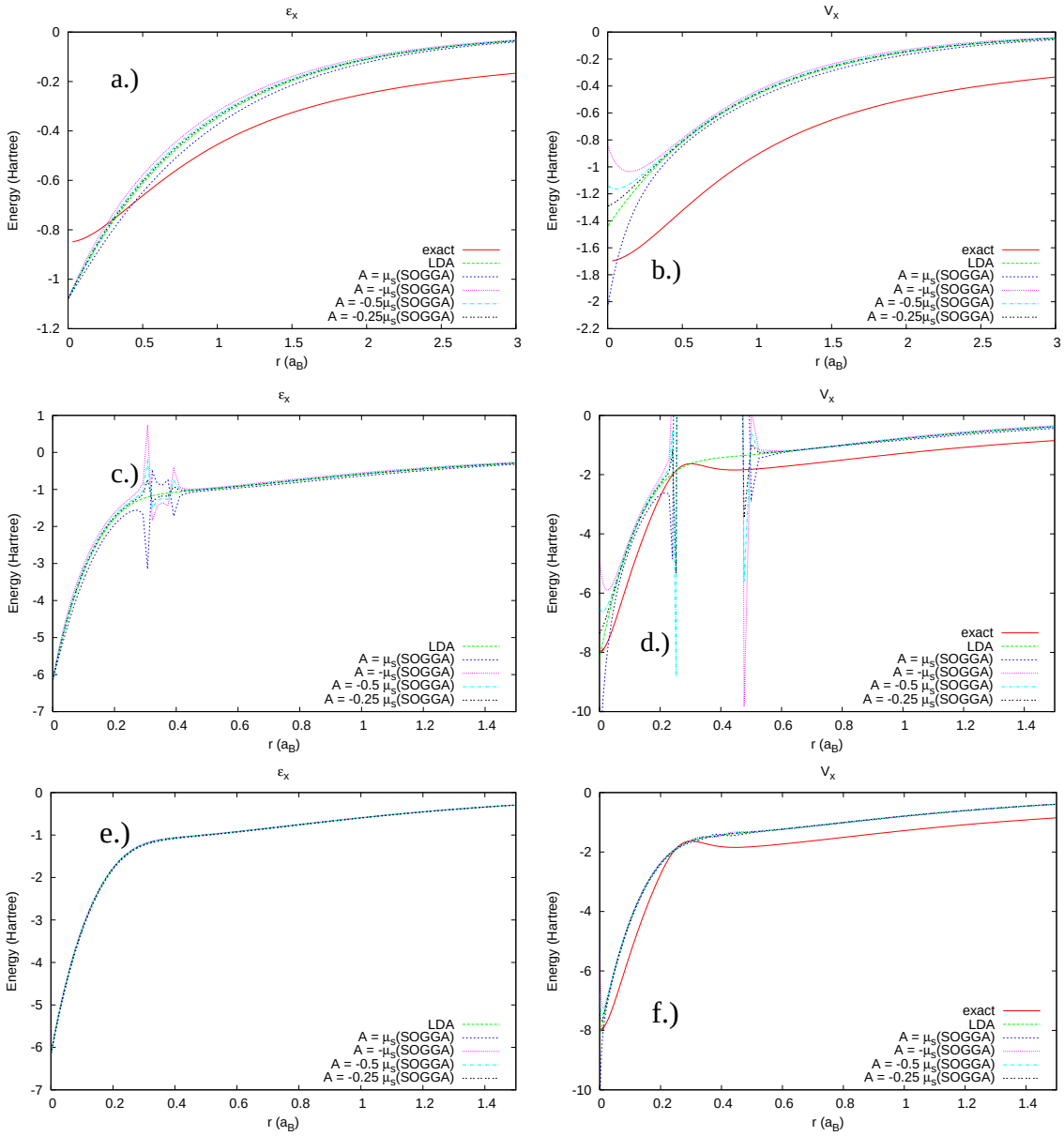

Figure 4.10: This graph shows the various uses of the advanced form. The various graphs show ϵ_x and V_x for He using $B = 2$ ((a) and (b) respectively), Ne using $B = 2$ ((c) and (d) respectively) and Ne using $B = 10$ ((e) and (f) respectively). For each plot the x-axis is radial distance and the y-axis is energy. For (a), (c) and (e) we can see that this advanced form is a very small correction from the LDA, seeing as how nearly every curve lies almost directly on the LDA (the big exception being in (c) where there are poles in each of the advanced forms). The difference is seen in (b), (d) and (f). There are four different A's used for each case. The only one that isn't negative is $A = \mu_s^{SOGGA}$.

Chapter 5

Discussion

5.1 Research Overview

DFT has been very useful in solid state computation. Unfortunately it is not yet trustfully predictive. Since DFT is so widely used, working on reaching for better functionals will be helpful for many people. Although we will not find the perfect universal functional, we can question whether we have truly exhausted our simple GGA options before moving on to more complicated methods. This research is being done to come up with a functional that moves in a direction of more predictive computational modelling with DFT in order to fulfill this narrowing goal.

We have many different ideas that have been tested out in this research. Table 5.1 is a list of all the functionals discussed in Chapter 4. The table contains the name given to the functional (a name such as simple-PBE means that the functional uses the simple form and the PBE parameters), the form of the functional, the μ_q used in the functional and the μ_s that it came from, the κ value used, the η value used (if it was the general form) and finally the M value used (if it was the cusp form). The final form (advanced) is the form listed in the Section 4.4. The values for A and B

Functional	Functional Form	μ_s	κ	η	M
simple-PBE	$1+\frac{\mu_q q}{\sqrt{1+\left(\frac{\mu_q}{\kappa}\right)^2 q^2}}$	0.21951	0.804	–	–
simple-SOGGA	$1+\frac{\mu_q q}{\sqrt{1+\left(\frac{\mu_q}{\kappa}\right)^2 q^2}}$	10/81	0.552	–	–
simple-rPBE	$1+\frac{\mu_q q}{\sqrt{1+\left(\frac{\mu_q}{\kappa}\right)^2 q^2}}$	0.21951	1.245	–	–
simple-PBEsol	$1+\frac{\mu_q q}{\sqrt{1+\left(\frac{\mu_q}{\kappa}\right)^2 q^2}}$	10/81	1.245	–	–
PBEq-PBE	$1+\frac{\mu_q q}{1+\frac{\mu_q}{\kappa} q}$	0.21951	0.804	–	–
general-SOGGA	$1+\frac{\mu_q q}{\sqrt{1+\eta q+\left(\frac{\mu_q}{\kappa}\right)^2 q^2}}$	10/81	0.552	$0<\eta<2\frac{\mu_q}{\kappa}$	–
cusp	$1+\frac{M}{q}$	–	–	–	$-\frac{2}{3}s_0^2$
advanced	$1+\frac{As^2}{Bs^2-q}$	–	–	–	–

Table 5.1: Various exchange enhancement factors used in this research. For the functional names, if there are multiple (e.g. simple-SOGGA)the first is the functional form and the second is the parameters used. Note: μ_s are values from literature and μ_q are three times that of μ_s. For the cusp functional we defined s_0^2 as the value of s^2 at $r = 0$ for He.

are not listed since various values were tried for each system.

All the results for He and Ne are plotted in Figure 5.1. We found through using the forms in Table 5.1 that our current ideas don't fix much of anything for an atomic system. The PBEq form introduces a new pole in the ϵ_x that wasn't there originally and makes the pole in the potential worse. When trying to fix the pole by introducing the square root and squared q term in the denominator for the simple form, the pole did in fact leave but a new problem was introduced: unphysical bumps and oscillations were produced farther out in ϵ_x and V_x respectively. Hoping to moderate these features, we tried to find a happy medium between the two by creating the general form and varying η from $\eta = 0$ (reproducing the simple form) to $\eta = 2\frac{\mu_q}{\kappa}$ (reproducing the PBEq form). Testing out $\eta = 1\frac{\mu_q}{\kappa}$ for a happy medium, we found that ϵ_x took the good from both the PBEq and simple forms, getting rid of the pole and reducing the bump farther out. The poor behavior for the general form came

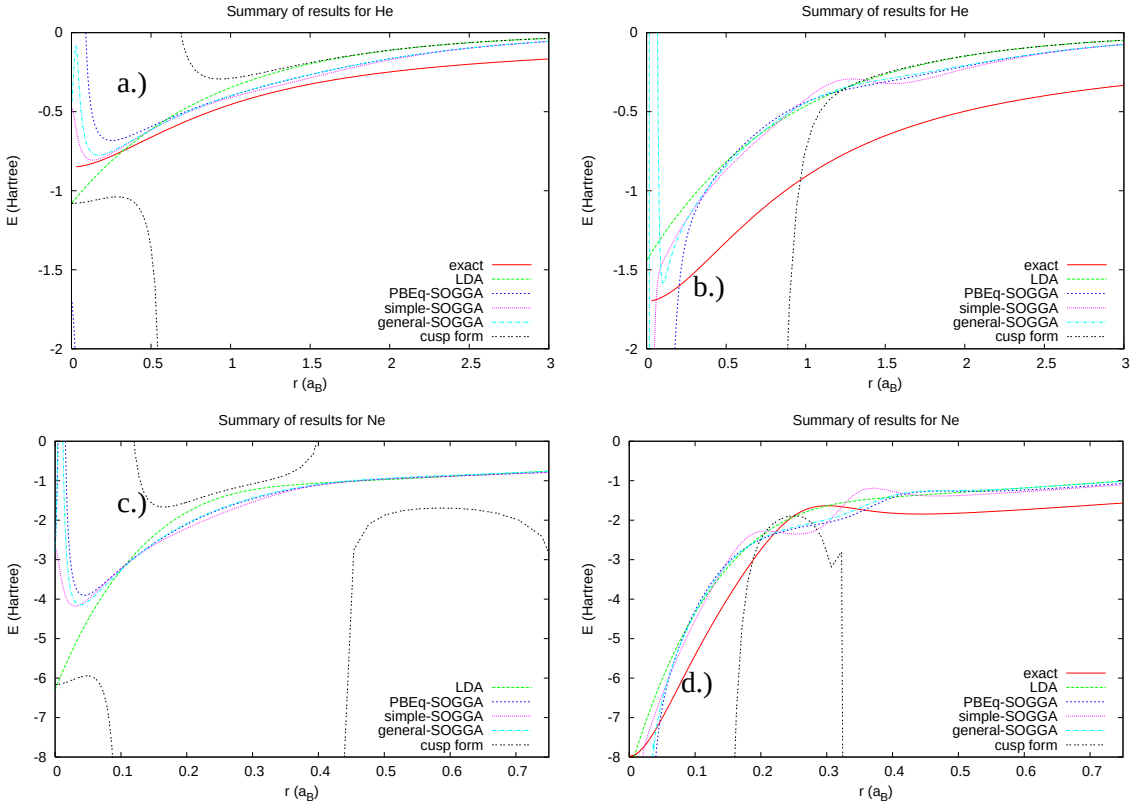

Figure 5.1: This is a plot of all the results from this research for both He and Ne. In (a) and (b) we have the results for He and in (c) and (d) we have the results for Ne. Likewise, (a) and (c) show the exchange energy per particle and (b) and (d) show the exchange potential, all versus r. The general form for both He and Ne are the optimized with η and α, but all others use the original (unmixed) form.

from V_x where, exactly the opposite of ϵ_x, it took the poor qualities of both the simple and PBEq forms. This gave the general form a poor cusp region, although with no pole, and kept the oscillations farther out, although better than they were with the simple form.

The cusp form was used to fix the cusp of ϵ_x to have the same behavior as the exact answer (namely that as $r \to 0$, then $\frac{d\epsilon_x}{dr} \to 0$, or more specifically that as $q \to 0$, then $\frac{d\epsilon_x}{dr} \to 0$). This definitely fixes the behavior for He for the cusp, although it produces a pole right around $r = 0.5a_B$. This also doesn't help to fix the potential at all either,

Functional	Atom	η	α	I	E_x	discussion
general-SOGGA	He	1.6	–	0.001547	-0.90035	
generalmix-SOGGA	He	1.6	0.63	0.000365	-0.92887	
PBE(s^2)-PBE	He	–	–	0.032629	-1.01795	
LDA	He	–	–	0	-0.88344	
exact	He	–	–	–	-1.02573	see reference [34]
general-SOGGA	Ne	1.9	–	0.001564	-11.2903	
generalmix-SOGGA	Ne	1.9	0.86	0.001531	-11.2915	
PBE(s^2)-PBE	Ne	–	–	0.127345	-11.0739	
LDA	Ne	–	–	0	-11.0237	
exact	Ne	–	–	–	-12.1139	see reference [34]

Table 5.2: The effect of optimization for various functional forms. This table includes the optimal parameters and the integral values that correspond to them as well as the total exchange energy. They are also compared to the PBE functional that utilizes s^2, the LDA result and the exact answer.

and it actually makes it worse. This form may actually produce a limiting case for more general functionals. The advanced form seems to work for He and Ne, although different values for A and B are chosen, making the functional not universal. Since we have not looked at anything other than atoms, this may only work for atomic systems as well as it does.

Table 5.2 contains a list of the best results we obtained for the general case from optimization for He and Ne and compares them to the PBE (original s^2 version), LDA and exact answers. The exact answer for He is discussed in 3.1 and the exact result for Ne was obtained from Umrigar [30]. We can see through using our optimization scheme, we were able to produce the best results for our functional. It is interesting to note that the general functional does not give the same optimized η or α value for both He and Ne, suggesting that there is something fundamentally wrong with using that form. It is also interesting to note that when used for He the optimized general form gives worse exchange energies than the PBE when compared to the exact, but when used for Ne the optimized general form gives better exchange energies than the

PBE. We seem to find that this minimization process does in fact help to find the best solution for what we're varying, although it doesn't give us encouraging results for our current functionals.

Through this research there was definitely not enough time to test every idea for functionals utilizing q in functionals. One thing that could be done is to try something for the mixing parameter α from Eq. (4.6) that utilizes how s^2 and q change. In this research we used a constant for α as a simple starting point, although it may be that nature prefers a more complicated way of mixing. Another thought would be that we could continue to try different ways to couple s^2 and q. In this research we tried coupling them through addition (seen through the use of $\bar{q}$) and division (used in the advanced form). Perhaps some sort of multiplication or exponential would be a better fit for the coupling. One other thing to try would be to see if there could be a form that benefits from completely separating s^2 and q from each other:

$$F_x(s^2, q) = 1 + g_x(s^2) + h_x(q) \tag{5.1}$$

It could be possible that using this sort of uncoupling of s^2 and q would produce a cancelling of poor behaviors.

5.2 Final Thoughts

During this research we have compared our results to exact theoretical calculation and Variational Monte Carlo simulation data. We had no experimental data to compare our results to, so this begs the question, "What is the use of this research if it isn't compared to experiment?". If we look at what kinds of quantities experiments obtain, it actually doesn't retrieve the exchange energy explicitly. The exchange-correlation

energy can be obtained, but this is quite hard if not impossible to separate into the exchange energy and correlation energy. Fortunately Filippi, Gonze and Umrigar [30] figured out how to separate the exchange and correlation energies through the Variational Monte Carlo simulation data by use of the known Kohn-Sham orbitals, which is something that is not obtained in experiments. Generally when a DFT calculation is compared to experimental data, it is through the application of the *total* energy to calculate bond lengths, atomization energies, ionization energies, bulk moduli, etc. Our code *exqlapl.py* as is does not do any calculations for DFT other than the exchange energy. If we wanted to compare our results to experimental data, we would also have to include calculations of the correlation energy, kinetic energy, external potential and Hartree energy and eventually return the total energy of the system. Once this is obtained we would make calculations for the ionization energies of He and Ne and see how those compare to experiment.

So if we are able to compare exchange-correlation energies to experiment, then why just look at exchange? The first answer to that question is that, compared to exchange, the correlation is a very small correction to the total energy. Another reason to focus on exchange before correlation is that correlation tends to cancel out part of the exchange energy. The correlation also tends to be a very complicated energy to deal with. We can see that the PBE form for the correlation enhancement factor H_c in Eq. 2.36 gives a very complicated logarithmic form for the enhancement factor.

Our research has been done to make sure that we have exhausted all of our simple options before truly relying on more complicated methods. We had ideas to test for a more simple model than the ones currently being employed hoping to determine whether they give a better result than the current GGA's used in the Jacob's Ladder. We have seen that our current ideas are not going to improve on our results, however

it is possible some of our other ideas may prove useful. At this point it looks like a combination of s^2 and q will most likely produce the best result for GGA's.

Bibliography

[1] Ivan Amato. Quantum chemistry for the masses. *Science*, 282:611, 1998.

[2] Stefano Baroni, Stefano deGironcoli, and Paolo Dal Corso, Andrea aand Giannozzi. Phonons and related crystal properties from density-functional perturbation theory. *Rev. Mod. Phys.*, 73:515–562, 2001.

[3] T. Jungwirth, Jairo Sinova, J. Masek, J. Kucera, and A. H. MacDonald. Theory of ferromagnetic (iii,mn)v semiconductors. *Rev. Mod. Phys.*, 78:809–864, 2006.

[4] Yaroslav Tserkovnyak, Arne Brataas, Bauer Gerrit E. W., and Bertrand I. Halperin. Nonlocal magnetization dynamics in ferromagnetic heterostructures. *Rev. Mod. Phys.*, 77:1375–1421, 2005.

[5] R. G. Endres, D. L. Cox, and R. R. P. Singh. Colloquium: The quest for high-conductance DNA. *Rev. Mod. Phys.*, 76:195–214, 2004.

[6] Stephanie M. Reimaann and Matti Manninen. Electronic structure of quantum dots. *Rev. Mod. Phys.*, 74:1283–1342, 2002.

[7] John P. Perdew, Kieron Burke, and Matthias Ernzerhof. Generalized gradient approximation made simple. *Physical Review Letters*, 77:3865–3868, 1996.

[8] John P. Perdew, Adrienn Ruzsinszky, Gábor I. Csonka, Oleg A. Vydrov, Gustavo E. Scuseria, Lucian A. Constantin, Xiaolan Zhou, and Kieron Burke. Restoring the density-gradient expansion for exchange in solids and surfaces. *Physical Review Letters*, 100:136406, 2008.

[9] Yingkai Zhang and Weitao Yang. Comment on 'generalized gradient approximation made simple'. *Physical Review Letters*, 80:890, 1998.

[10] B. Hammer, L. B. Hansen, and J. K. Nørskov. Improved adsorption energetics within density-functional theory using revised Perdew-Burke-Ernzerhof functionals. *Physical Review B*, 59:7413–7421, 1999.

[11] Yan Zhao and Donald G. Truhlar. Construction of a generalized gradient approximation by restoring the density-gradient expansion and enforcing a tight Lieb-Oxford bound. *Journal of Chemical Physics*, 128:184109, 2008.

[12] Antonio C. Cancio and M. Y. Chou. Beyond the local approximation to exchange and correlation: The role of the Laplacian of the density in the energy density of Si. *Physical Review B*, 74:081202, 2006.

[13] L. H. Thomas. The calculation of atomic fields. *Mathematical Proceedings of the Cambridge Philosophical Society*, 23:542–548, 1927.

[14] Carl Trindle and Donald Shillady. *Electronic Structure Modeling: Connections Between Theory and Software*. CRC Press, 2008.

[15] Richard M. Martin. *Electronic Structure: Basic Theory and Practical Methods*. Cambridge University Press, 2004.

[16] P. Hohenberg and W. Kohn. Inhomogeneous electron gas. *Physical Review*, 136:864–871, 1964.

[17] W. Kohn and L. J. Sham. Self-consistent equations including exchange and correlation effects. *Physical Review*, 140:1133–1138, 1965.

[18] Charles Kittel. *Introduction to Solid State Physics*. John Wiley & Sons, 2005.

[19] D. M. Ceperley and B. J. Alder. Ground state of the electron gas by a stochastic method. *Physical Review Letters*, 45:566, 1980.

[20] John P. Perdew and Karla Schmidt. Jacob's ladder of density functional approximations for the exchange - correlation energy. *AIP Conference Proceedings*, 577:1–20, 2001.

[21] P. R. Antoniewicz and Leonard Kleinman. Kohn-sham exchange potential exact to first order in $\rho(k)/\rho_0$. *Phys. Rev. B*, 31:6779–6781, 1985.

[22] K. Capelle Mariana M. Odashima. How tight is the Lieb-Oxford bound? *J. Chem. Phys.*, 127:054106, 2007.

[23] Garnet Kin-Lic Chan and Nicholas C. Handy. Optimized Lieb-Oxford bound for the exchange-correlation energy. *Phys. Rev. A*, 59:3075–3077, 1999.

[24] K. Capelle Mariana M. Odashima. Empirical analysis of the Lieb-Oxford bound in ions and molecules. *Int. J. Quantum Chem.*, 108:2428, 2008.

[25] Jianmin Tao, John P. Perdew, Viktor N. Staroverov, and Gustavo E. Scuseria. Climbing the density functional ladder: Nonempirical meta–generalized gradient approximation designed for molecules and solids. *Phys. Rev. Lett.*, 91:146401, 2003.

[26] C. R. Hsing, M. Y. Chou, and T. K. Lee. Exchange-correlation energy in molecules: A variational quantum Monte Carlo study. *Phys. Rev. A*, 74:032507, 2006.

[27] Maziar Nekovee, W. M. C. Foulkes, and R. J. Needs. Quantum Monte Carlo analysis of exchange and correlation in the strongy inhomogeneous electron gas. *Phys. Rev. Lett.*, 87:036401, 2001.

[28] Aaron Puzder, M. Y. Chou, and Randolph Q. Hood. Exchange and correlation in the Si atom: A quantum Monte Carlo study. *Phys. Rev. A*, 64:022501, 2001.

[29] J. C. Slater. Atomic shielding constants. *Phys. Rev.*, 36:57–64, 1930.

[30] C. J. Umrigar C. Filippi, X. Gonze. Generalized gradient approximations to density functional theory: comparison with exact results. *Recent Developments and Applications to Density Functional Theory*, 4:295, 1996.

[31] Neal Coleman. Report on uniform/nonuniform grids, stos and approximations, 2009. unpublished report.

[32] Neal Coleman. Report on polynomial interpolation, 2009. unpublished report.

[33] John David Jackson. *Classical Electrodynamics*. John Wiley & Sons, 1999.

[34] J. P. Perdew and Alex Zunger. Self-interaction correction to density-functional approximations for many-electron systems. *Physical Review B*, 23:5048–5079, 1981.